Solid-state and polymer nanopores for protein sensing: a review

Nathan Meyer, Imad Abrao-Nemeir, Jm Janot, Joan Torrent, Mathilde Lepoitevin, Sebastien Balme

Solid-state and polymer nanopores for protein sensing: a review

Nathan Meyer[ab], Imad Abrao-Nemeir[a], Jean-Marc Janot[a], Joan Torrent[b], Mathilde Lepoitevin[c], Sebastien Balme*[a]

[a] Institut Européen des Membranes, UMR5635 UM ENCSM CNRS, Place Eugène Bataillon, 34095 Montpellier cedex 5, France.

[b] INM UM, CNRS, INSERM, Place Eugène Bataillon, 34095 Montpellier cedex 5, France.

[c] Institut des Matériaux Poreux de Paris (IMAP), UMR 8004 CNRS, Ecole Normale Supérieure de Paris, Ecole Supérieure de Physique et de Chimie Industrielles de Paris, PSL Université, 75005 Paris, France

* Corresponding Author: Sebastien.balme@umontpellier.fr

Abstract

In two decades, the solid state and polymer nanopores became attractive method for the protein sensing with high specificity and sensitivity. They also allow the characterization of conformational changes, unfolding, assembly and aggregation as well the following of enzymatic reaction. This review aims to provide an overview of the protein sensing regarding the technique of detection: the resistive pulse and ionic diodes. For each strategy, we report the most significant achievement regarding the detection of peptides and protein as well as the conformational change, protein-protein assembly and aggregation process. We discuss the limitations and the recent strategies to improve the nanopore resolution and accuracy. A focus is done about concomitant problematic such as protein adsorption and nanopore lifetime.

1. Introduction

Proteins are key macromolecules in life. They play numerous roles from mechanical support to signal transport. Their precise conformation provides their function and govern their interactions with other molecules. Proteins have complex structures that are necessary to characterize to elucidate their properties. This is complex because of the large number of amino acids, their highly variable physicochemical properties (hydrophobicity, charge density size), as well as the three-dimensional structure of protein including the folding and oligomerization. [1]. However, a large class of proteins or peptides do not exhibit a specific 3D structure as the intrinsically disordered proteins (IDP) involved in degenerative pathologies such as Parkinson's or Alzheimer's diseases.

The folding/unfolding or conformational changes are also important since they provide the protein's function. The protein folding can be represented as an energy landscape [2,3] meaning that they can co-exist under different structures at equilibrium [4,5]. One challenge is the characterization of such energy map of protein folding including the dynamic aspect of conformational change [6,7]. Protein-protein interactions are also a key point of their functionality. This involves the oligomerization and aggregation as for example the amylogenesis [8,9]. In this case, the identification of different populations of protein aggregates as well as the access of kinetic information is highly challenging. Another question that conventional techniques cannot answer is the state of the protein during the lag phase corresponding to the early phase of protein aggregation prior to amyloid growth [10,11]. The characterization of protein-protein interactions requires miniaturized techniques allowing the assay with a minimal sample consumption and low-cost such as microfluidic platforms [12]. As for the protein folding/unfolding, the point of interest is the access of information about the dynamic of protein interactions.

So far, there are numerous techniques for characterizing peptides and proteins, including ELISA [13], mass spectrometry [14], fluorescence spectroscopy [15], real-time PCR using chimeric protein covalently linked to ssDNA [16] and immuno-staining [17]. All these conventional techniques suffer from limitations. The information is obtained for ensemble averaging (conversely that single molecule) that could hide the information about different populations in a sample. The conventional technique can require high concentration and not suitable to detect several copies. Otherwise, ultra-sensitive techniques like fluorescence require labelling with fluorescent dye that can influence the protein properties. The protein sensing often necessitates labour-intensive and large amount of chemical or consumable sample preparations to extract the target. Finally, the protein analysis is performed by costly facilities such as mass spectroscopy, NMR or fluorescence. .

Single nanopore sensing was demonstrated for DNA sensing using α-hemolysin in 1996 [18]. For the past three decades, a large research effort has made possible the commercialization of DNA sequencers [19,20] and more recently the first proof of concept in protein sequencing [21–25]. More generally, the nanopore technology has emerged as a powerful alternative method due to its intrinsic capability of single molecule detection at ultra-low concentrations [26,27]. At femtomolar concentrations, the time between the detection of two consecutive biomolecules is in the minutes range [28]. In addition, the technique is label-free, thus do not require expensive detection kits making the sample preparation easy. Last but not least, the nanopore can be included into a high-throughput device for the detection of multiple analytes [29,30] . In the past three decades, many types of nanopore have been investigated including biological pores made of bacterial toxins forming pores, wild type and mutants [31], and solid-state nanopore[32,33] . Biological

nanopores possess an excellent low noise level [34,35]. Their structures are extremely precise and providing a high reproducibility of the results. The biological nanopore and their mutants have characteristics in terms of size, gating behaviours, and charge properties that can be individually exploited for different sensing applications[25,36–38]. However, they mainly present a low range of diameter making impossible the detection of large folded protein or oligomer except by bumping or trapping [39,40]. Indeed it is difficult to expand the pore diameter of a biological channel [41]. Due to the need for tunable nanopores with better stability, easy to design and tune surface chemistry, solid-state nanopores emerged within different materials such as silicon based [42,43], 2D materials [44], glass nanopipette [45,46] and track-etched nanopores [47].

In this review, we will give a broad overview of the protein sensing using solid-state and polymer nanopores. A section will be specifically dedicated to introducing all these nanopores with a focus on the surface chemistry that is a key point for protein sensing. Then, we will consider the protein sensing regarding the technique of detection: the resistive pulse [48,49] and ionic diodes [50,51]. For each strategy, we will discuss their limit and the future to improve the nanopore resolution and accuracy. We also discuss about concomitant problematic such as protein adsorption and nanopore lifetime. The up-to-date methods allowing the improvement of the single protein detection and identification including surface functionalization, crowding effect and machine learning will be presented.

2. Nanopore design

2.1. The different types of solid-state and polymer nanopore

Techniques to produce solid-state nanopores include, high-energy-beam nanofabrication tools, such as focused ion beam, gallium ion milling or electron beam and laser-assisted puller. The solid-state nanopore can be classified according to their material, aspect ratio and geometry.

Nanopore with a low aspect ratio. Such nanopore are typically drilled inside a thin film (10 to 30 nm thickness) of a semiconductor material. Originally, the material was the stressless SiN drilled by a focused ion beam (FIB) or a transmission electron microscope (TEM) beam(Figure 1a-b) [52–54]. More recently other materials like HfO_2 was considered due to its lower noise level [55]. The nanopore diameter can be easily tunes from 2 nm to tens nanometres. However, sub-nanometre nanopore can be drilled in SiN or MoS_2 [56,57] In terms of surface chemistry, the silicon nitride is hydrophobic. However, to ensure their wettability, they undergo oxidative treatment using piranha solution, O_2 plasma or ozone[58]. This creates silanol moieties at the surface to ensure a better wettability and also suitable for silanization chemistry [59,60]. In that case, the external and inner nanopore surface are supposed chemically equivalent. One major problem of such nanopore is the difficulty to fill nanopore with aqueous solution and the requirement to expensive facilities for the drilling. To overcome these problems, the dielectric breakdown technique has emerged as a cheap and easy to use alternatives to drill nanopore from 2 nm to 15 nm (Figure 1c and 1ed) [42,61]. A year ago, a commercially available device was launched allowing automatizing such nanopore fabrication with a good reproducibility [62]. Coupled with a laser beam irradiation (Figure 1d and 1-f), a nanopore with a diameter about 50 nm can be achieved[63]. Nevertheless, this method can conduct to drill irregular nanopore of multiple pore formation when the process is not fully

controlled[64] . In addition, in such nanopore the inner pore surface is not well defined and it is likely chemically different from the external one.

Despite the success of solid-state nanopores in sensing various types of biomolecules, surface charge density, wettability, chemical groups, adsorption of contaminants are extremely difficult to control. Their low signal/noise ratio is a problem for high quality sensing. Another disadvantage of SiN is their stability during the experiment. Indeed, the raw SiN surface after the fabrication has to be activated to ensure the wettability. However, the vicinal silanol created on the surface condensate to form Si-O-Si inducing surface stage changes and bubble nucleation[65,66] . In order to reduce the length of the nanopore and thus expect to reach the resolution of the biological nanopore[67]. To this end, 2D-materials such as graphene[68] , boron nitride[69] , MoS_2[70] or metal transition carbide MXene[71] are deposited on silicon substrate and drilled by TEM, STEM or chemical etching.

Nanopipette. Nanopipettes have the unique advantages of low-cost fabrication process[46]. They are obtained in a few seconds by pulling quartz capillary with a pipette puller instrument (Figure 1g-h). Additionally, the size and geometry of nanopipettes can be fine-tuned by adjustment of fabrication parameters, and integration of nanopipettes with positioning systems. Nanopipette possess low-noise performance, chemical stability, easier handling, high-aspect ratio geometry and simple routes for multiplexed sensing. Although, it is possible to tune the pore dimensions, pore diameters below 20 nm are difficult to achieve without additional facilities. The geometry of nanopipette is conical exhibiting an

angle about several degrees[72]. In terms of chemistry, the quartz allows classical silanization chemistry as well as certain polyelectrolyte assembly [72,73].

Polymer nanopore. Compared to silicon and glass based inorganic materials, polymer membranes can be an alternative. The ion-tracking fabrication is easy to use, polymers are low-cost materials, they have a wide range of physico-chemical properties, and their surface can be modified. The increasing interest for single nanopores in polymer track-etched membranes is due to their unique properties including uniform pore size and length, tunable pore geometry, and an easy surface functionalization, and high stability over time. The track-etching of membranes is done in two steps: (i) the swift heavy-ion irradiation and (ii) the chemical etching of latent ion tracks in polymers (Figure 1i-k). Among the various techniques, ion track technology permits control over the number of pores per square centimetres of the polymer surface (from single to multipore membranes), dimensions and shape (cylindrical, conical, cigar-shaped...) [74–76]. It has been found that asymmetric nanopores are cation selective and have diode-like voltage-current characteristics. The possibility to manufacture cylindrical and conical nanopore following the same condition, it is possible to know exactly the number of carboxylate moieties after opening thus, the yield of surface grafting [77]. Despite advantages like chemical stability and the easy filling, they suffer from numerous limitations.Getting the exact dimensions and controlling *a priori* the tip size for a conical nanopore are difficult.

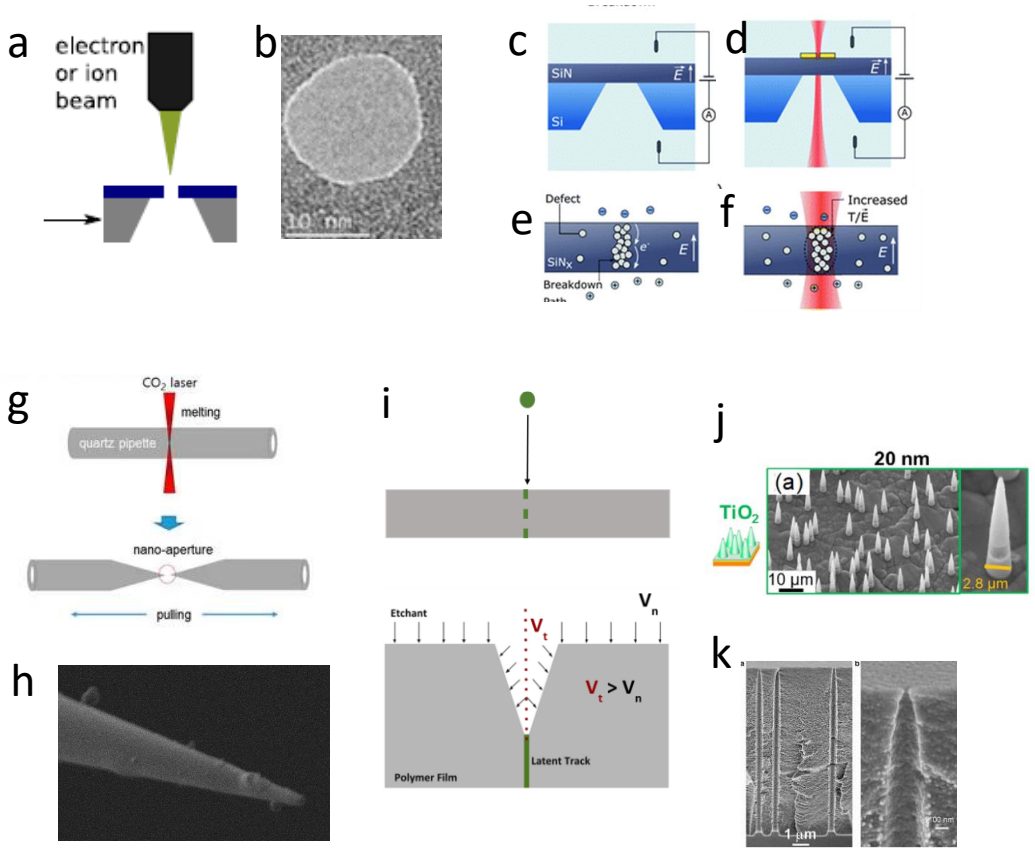

Figure 1: (a) Sketch of SiN nanopore drilled using electron or ion beam Reproduced with permission [78], 2017, Elsevier (b) TEM image of a SiN nanopore. Illustration of classical (c) and laser-assisted (d) dielectric breakdown and the distribution of defects inside the SiN film (e) and (f) respectively, Reproduced with permission [42], 2021, American Chemical Society (g) sketch of nanopipette pulling [79] and (h) SEM image of a nanopipette. (i) sketch of track-etching technique Vt and Vn are the speed of chemical etching inside the irradiated zone and bulk material respectively (j) replica of conical nanopore obtain by TiO_2 deposition by atomic layer deposition [80] (k) FESEM image of "bullet-like" shape nanopore, Reproduced with permission [81], 2009, Elsevier

2.2. How to choose the appropriate nanopore?

The nanopore sensing is based on electric*al ion-current measurement*s. In a typical experiment, the nanopore is placed between two reservoirs filled with an electrolyte solution where are immersed Ag/AgCl electrodes. Then the current generated by an electrolyte that crosses through the nanopore under applied voltage is recorded at the function of the time. To date, two techniques are utilized for protein sensing. The first one is the resistive pulse sensing (RPS). In this case, the protein detection is due to the current perturbation caused by its interaction with the nanopore through translocation or bumping

events. The second one is the ionic current rectification (ICR) that involve asymmetric nanopore. In that case, the sensing of the analyte is due to a change of charge on the nanopore inner wall. In the next section, both the RPS and ICR are detailed. The table 1 summarizes the essential information to choose the suitable nanopore as function of the detection mode.

Table 1 : Comparison of different types of nanopore

Nanopore type	Material	Size	Lifetime	Detection mode	Resolution
Solid-state	SiN, SiO, HfO_2	> 2 nm	Raw (days) Functionalized (weeks)	RPS	***
Nanopipette	Quartz	> 20 nm > 5 nm	Raw (days) Functionalized (weeks)	RPS ICR	*** **
polymer	PET, PC, PI, Kapton	> 2 nm (conical) > 20 nm (bullet shape and conical	Raw (weeks) Functionalized (months)	RPS ICR	* ***

3. Protein detection using ionic current rectification

3.1. Principle of ionic diode

The ionic current rectification (ICR) is an alternative method for protein detection using single nanopore. It requires use of a nanopore with asymmetric geometry and surface charge (Figure 2a). Inside such nanopore, the asymmetric distribution of the electrolyte induces a non-Ohmic (nonlinear regime) current response as a function of applied voltage[82–84] . In this case, the I-V curve shows a current rectification similar to the response of a diode [83,85–88]. Such ionic diode properties are the strength of asymmetric track-etched nanopore (i.e, bullet-shape or conical). The nanopipette has also ionic diode properties due to their asymmetric shape[89]. The ICR is extremely sensitive to the surface modification and both the track-etched nanopore and nanopipette are easy to functionalize and thus were widely used to design specific sensor[78,90]. In order to provide a quantitative description of the IRC, the authors define the rectification factor noted R_f as the ratio of current measure usually at V= ± 1 V or more[91] .

Generally speaking, the current rectification depends on the nanopore shape and the surface charge (density and distribution) [92]. As an example, the alternating deposition of polyelectrolyte layers of poly-L-lysine (PLL) and poly(styrene-sulphonate) or by polyethylenimine and chondroitin-4-sulfate (ChS) can be followed in real time by the inversion of current rectification because of a change of surface charge of the pore [93–95]. Similar behaviour was reported by deposition of chitosan and polyacrylic acid (PAA) to detect metal ions using nanopipette and polymer nanopore [96,97]. The modification with PLL grafted with poly(ethylene glycol) (N-hydroxysuccinimide 5-pentanoate) ether 2-(biotinylamino) ethane (NHS-mPEG-biotin) made it possible to attach or recognize biotin-binding proteins [94]. The comparison of I–V responses prior to and following introduction of analyte molecules provides a way for molecular detection [98–100]. The

biorecognition can be identified from the change of ionic current rectification when a target biomolecule interacts with a ligand grafted inside the nanopore [73,101–106]. The ligands are immobilized inside the nanopore via self-assembly or covalent surface grafting (i.e., carbodiimide moieties or silanization). In this context, nanopore have been engineered to improve the ionic current rectification for the specific detection of a variety of peptides and proteins [78,107].

3.2. Application of ICR on protein sensing

3.2.1. Peptide and polypeptides

Ionic diodes are considered for peptide detection. They have the advantage to regulate the ICR as a function of the pH and thus the charge of an amino acid inside nanopore as shown for the lysine [108]. The functionalization of inner surface wall with BSA was proposed as an efficient way for stereo-selective detection of tryptophan (Trp) [109]. As previously mentioned, the polyelectrolyte adsorption is directly characterized by an inversion of the ICR.

3.2.2. Protein sensing by ICR

The simplest way to specifically detect one protein is to play with the affinity for the nanopore surface. It was shown that BSA can be detected using raw nanopore as well as after functionalization with amine or aliphatic moieties. The main difference of the different functionalization is the amplitude of current rectification induced by the BSA adsorption [110,111]. Several proteins were specifically detected using conical or cylindrical functionalized nanopore. Among the specific function, the aptamer are short polynucleotide strands used for nanopore sensing due to their specificity for a substrate [112]. They were used to specifically detect lysozyme using polymer nanopores (Figure

2b) and nanopipettes [105,113]. One interesting property of aptamers is the reversibility of their binding with protein such as thrombin allowing the reusability of the sensor [106]. The grafting of a probe inside the nanopore is another way for the detection of a specific protein. This was illustrated by Ali *et al.* who grafted mannose inside a conical polymer nanopore to detect the concavalin A [114] . The specificity of the sensing was demonstrated against lysozyme and bovine serum albumin.

Another strategy is to use protein-protein affinity. The concavalin A was detected with a complex functionalization involving HRP-enzyme and mannose (Figure 2c) [104]. A more complex system based on multilayer of protein was also reported. Cylindrical nanopores were functionalized with nanolaminate deposition of ZnO and Al_2O_3 to optimize the diameter. Then a PEG-biotin was grafted to specifically bind avidin or streptavidin. Such nanopore also exhibits an interesting pH gating properties [115]. After addition of polyethylene glycol grafted bovine serum albumin (PEG–g-BSA), the anti-BSA antibody was detected at an optimal pH of 6 and 7. This investigation reveals the influence of the spacer on the ionic current rectification and thus the efficiency of antibody or IgG detection [116]. Finally, this strategy is interesting since the concentration of protein needed for detection is around 1 nM and does not require fluorescence labelling. However, lower protein concentration could be reached since only a partial modification of the nanopore is required to modify the IRC [92]. Thus in a theoretical point of view, the concentration limits are determined by the diffusion of the protein to reach the nanopore and the constant of association between the protein and the ligand grafted inside the nanopore.

The electrostatic interactions are also a way to functionalize conical PET nanopore. The deposition of poly(allyl amine hydrochloride) (PAH) functionalized with biotin allows to

specifically detect avidin and streptavidin [101]. The poly-l-lysine grafted polyethylene glycol biotin (PLL-g-PEG-biotin) was also proposed to detect avidin (Figure 2d). The interest of this approach is that the functionalization is totally reversible allowing the re-use of the nanopore [94]. One of the key aspects of using antibodies is the ability to create multiplex detection. Duan and Yobas developed a multiplex nanopore platform using a microfluidic channel for the detection of three cancer biomarkers, carcinoembryonic antigen (CEA), AFP, and Human Epithelial Receptor 2 (HER2). First, the nanopore and microchannels were etched onto a silicon wafer using photolithography. Then the glass nanopores were functionalized with different antibodies by silane chemistry. The multiplex then used current rectification to measure the concentrations of each biomarker. First, the multiplex was tested only for the detection of cardiac Troponin T (cTnT), a cardiac biomarker, in buffer solution. The nanopore biosensor was able to detect cTnT at a concentration as low as pM. This was then followed by the multiplex detection of the three mentioned cancer biomarkers, their detection was carried out first in the buffer between 0.02 to 200 pM , then in human serum at concentrations from 2 pM to 200 pM [117].

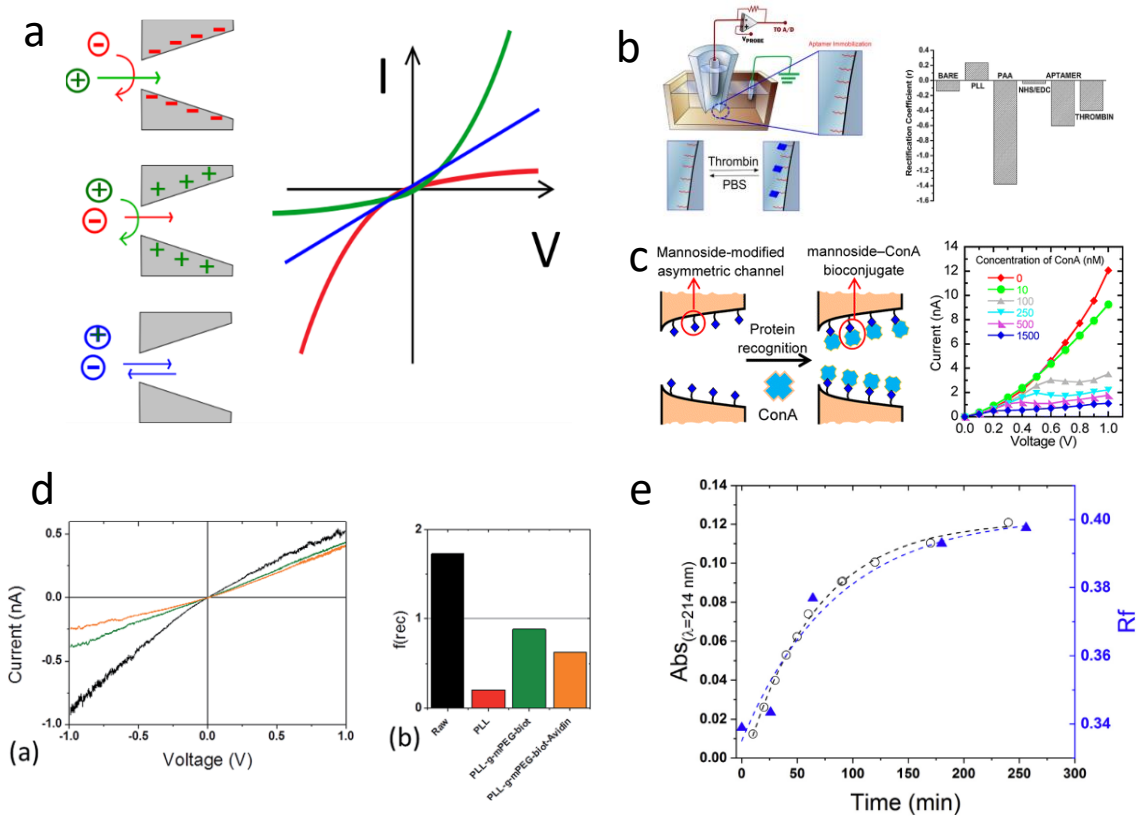

Figure 2 : (a) Sketch of the correlation of surface charge and IRC in asymmetric nanopore. Right illustration of ion selectivity as a function of surface charge. Left, illustration of associated IV curve for negative (red line), neutral (blue line) and positive (green line) surface charge (b) Sketch of experimental set-up and the binding of thrombin on the STING sensor functionalized with aptamers taken. Right, electrochemical measurements (rectification factor) evidencing the functionalization of the STING sensors, Reproduced with permission [106],2011, Elsevier (c) detection of concanavalin A by polymer conical nanopore functionalized with mannose. Right Sketch of experimental set-up and the binding of concanavalin A. Left, IV curves recorded at various concentration concanavalin A from 0 nM to 1.5 µM, Reproduced with permission [114], 2013, American Chemical Society. (d) detection of avidin by polymer conical nanopore functionalized using self-assembly PLL-g-PEG-biotin. The subpanel -a- IV curves recorded for the raw nanopore (black) after the deposition of PLL-g-PEG biotin (green) and after avidin (orange). Subpanel -b- associate rectification factors, Reproduced with permission [94], 2016, Royal Society of Chemistry. (e) kinetic of heparin degradation by heparinase follow by classical UV method (black circle) and conical nanopore functionalized with poly-L-lysine (PLL) (blue triangle), Reproduced with permission [90], 2019, Elsevier. Note that the figure b is nanopipette while the figures e,d,c the nanopore are polymer with a conical geometry

3.2.3. Probing enzymatic reaction by ICR

The conical nanopore can serve to detect or investigate the protein properties like enzymatic degradation or affinity with a substrate following several strategies. First, the nanopore can be functionalized with a substrate. Ali *et al.* have grafted inside the nanopore glycine *p*-nitroanilide - and aminohexanoylacetylcholinesterase O-(6-)-choline substrate. The enzymatic degradation of these molecules was characterized by an inversion of the

current rectification[118]. A nanopore decorated with enzymes inside its pore can be an interesting strategy for sensing. Horseradish peroxidase was grafted to detect H_2O_2 [119]. The calmodulin was grafted inside a nanopipette allowing determining its affinity constant of about $6.3 \pm 0.8 \times 10^{-5}$ M [120]. The kinetic of degradation of heparin by heparinase was measured using a conical nanopore functionalized with poly-L-lysine. The kinetic constant was found similar to the one measured with classical methods based on UV absorbance (Figure 2e). Such strategy was developed to detect the over-sulfated chondroitin sulfate due to its ability to inhibit the heparinase [90]. In this work, the kinetic constant obtained by nanopore is close to the one measured with classical method. Pérez-Mitta *et al.* used the dependency of the ionic transport properties of nanofluidic devices on the sign and magnitude of their surface charges to enhance the signal of urease inside a nanopore. This concept was tested first by using a PET conical nanopore that was functionalized with poly (allyl amine) through electrostatic interactions in order to test the amplification signal for measuring the pH inside the nanofluidic channel. This was then followed by immobilizing urease inside the nanopore. This has allowed for the tailoring of the ionic current through the concentration of the urea in the channel and thus making the concept a highly sensitive urea sensor with excellent repeatability and reproducibility with a limit of detection reaching 1nM [121].

4. Protein detection using resistive pulse

4.1. Resistive pulse technique

Resistive pulse sensing (RPS) uses the Coulter principle developed in the 1950s for the counting erythrocyte translocation through a micrometer-sized hole [122]. The first application using a nanometre-size hole was demonstrated by Bezrukov *et al.* for sensing

single polymers in solution through an alamethicin channel [123]. A few years later, Kasianowicz *et al.* detected for the first time polynucleotide molecules through an α-hemolysin [18]. The RPS is a single molecule technique consisting to apply a constant voltage across a single nanopore using two Ag/AgCl electrodes (Figure 3a). It results in a steady-state ion current due to the flow of ions across the nanopore. In the general case, the ionic current in a pore at a high ionic strength (>100 mM) can be approximated using eq. (1)..

$$i_0 = \frac{V}{R_0} = V\sigma\frac{\pi d^2}{4l} \qquad (1)$$

where V is the applied voltage, d is the pore diameter, l is the length of the membrane or nanopore thickness, σ is the conductivity of the electrolyte in bulk solution and R_0 is the resistance of the nanopore. For a nanopore with a nm scale length, the access resistance is in the same order of magnitude as the nanopore one. Thus, the current is generally expressed as

$$i_0 = (\mu_+ + \mu_-)ne(\frac{4l}{\pi d^2} + \frac{1}{d})^{-1}V \qquad (2)$$

where μ_+ and μ_- are the electrophoretic mobility of ions, n is the number density ions.

As individual analyte molecules translocate through or interact with the pore, the transient state induces a perturbation of the ionic current (Figure 3b). Depending on the nature of the analyte and the ionic concentration inside the pore, the perturbation can be a current blockade or enhancement [124,125]. For proteins, current blockades are generally reported except in the case of highly charged and intrinsically disordered proteins such as the

activation domain from the p160 transcriptional co-activator for thyroid hormone and retinoid receptors and the nuclear co-activator-binding domain of CREB-binding protein [126] or Aβ(1-42) [127]. The current perturbations called "event" are usually characterized by the amplitude, the duration, and a capture rate frequency. They depend on the characteristics of the analyte, the nanopore, the nature of the electrolyte as well as the interactions that take place between the analyte and pore wall (Figure 3b). Typically, for a protein, the relative current blockade ($\Delta I/I_0$) depends on the volume, the shape and the charge of the object as well as the concentration and the nature of the electrolyte. The dwell time (Δt) depends on the charge and the diffusion coefficient of the object, but also on its interaction with the nanopore and the escape-free energy. It also gives information about the conformation adopted by the object inside the nanopore. The capture rate is relative to the diffusion coefficient and the concentration of analyte but also the free-energy barrier that the object has to overcome to enter the nanopore. This barrier depends on the length, the rigidity and the deformability of objects as well the nanopore properties.

To date, resistive pulse sensing is the most used technique for nanopore sensing. Beside DNA, it has been used for a wide range of analyte, including small molecules [128,129], nanoparticles [130–133], peptides [134–137], proteins [138–141], amyloids [142–144], nanoparticles and viruses [145–147]. The resistive pulse was also used to investigate the protein/nanoparticle interactions [148,149]. To impart specificity or to prevent the interactions between the protein and surface of synthetic pores, a wide selection of surface functionalization approaches can be used [78,150].

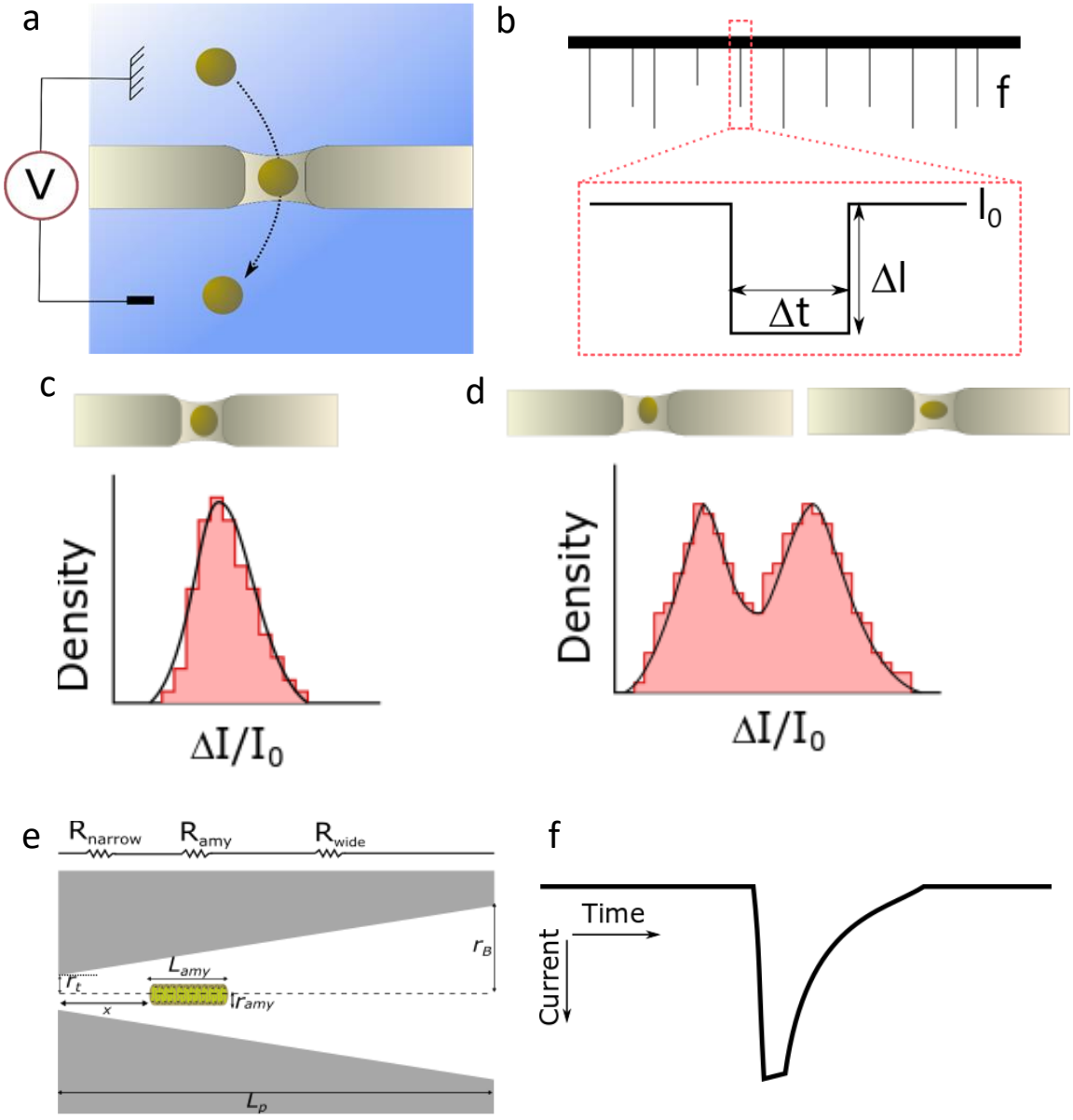

Figure 3:sketch of (a) resistive pulse technique and (b) the current recorded during an experiment with a zoom on current blockade. f is the capture rate, I_0 the nominal current, ΔI, the amplitude of the current blockade and Δt the dwell time. Illustration of proteins with different shapes inside a SiN nanopore for spherical (c) and spheroid (d) and the illustration of relative current blockade distribution showing one distribution for spherical shape protein and two distributions for spheroid that depend on the protein orientation inside the nanopore. (e) Scheme of amyloid translocation inside a conical nanopore, Reproduced with permission [151], 2018, American Chemical Society (f) illustration of asymmetrical shape of current blockade recorded during the translocation of fibres inside asymmetric nanopore (conical or bullet-shape, note several examples can be found in ref[152] .

4.1.1. Protein translocation

Proteins have both complex structure and heterogeneous charges distributed along their length. This suggests that particular orientation will be preferred to enter inside the

nanopore. The structure of the protein during translocation can be folded, partially unfolded, completely unfolded or aggregated [153,154]. This depends on their three-dimensional native-state structure and the conditions during the measurement. When the proteins translocate totally folded or unfolded, the segment exposed to the influence of the electric field inside the nanopore will be different. This can affect both the current blockade amplitude and dwell time. The RPS was used to determine the shape of individual proteins, which have length shorter than nanopore thickness. The amplitude of the current blockade is a function of protein volume, shape, and time-variant protein orientation during its translocation through the nanopore. At first approximation, the amplitude of the current blockade is correlated to the physical blocking volume of the protein over the sensing volume of the pore. It can be considered as the volume displacement of the electrolyte solution from the pore using a simple Ohm's law [155,156]. It can be basically approximated by the ratio of the molecular volume to the pore volume (equation 4)

$$\frac{\Delta I}{I_0} = f\frac{\Delta V_{mol}}{V_{pore}}S \qquad (3)$$

where *f* measures the molecular shape and orientation and S is a size factor that accounts for distortions in the electric field that occur when the molecule is comparable in size to the pore [157,158]. The most accurate correction factor $S\left({}^{d_m}\!/_{d_p}\right)$, where dm is the diameter of the molecule and dp is the diameter of pore was developed by Smythe [159] and Deblois [160] for all dm/dp as reported by Qin et al. [158].

$$S\left({}^{d_m}\!/_{d_p}\right) = \frac{1}{1-0.8\left({}^{d_m}\!/_{d_p}\right)^3} \qquad (4)$$

For a cylindrical pore and spherical protein, the equation 3 can be rewritten in the form [161–163]

$$\frac{\Delta I}{I} = \frac{-\pi V_A d_m^3}{4\rho(l_p+0.8d_p)^2} S \qquad (5)$$

where V_A is the applied voltage, ρ the resistivity of the electrolyte solution and lp the length of the nanopore. The volume exclusion model has yielded accurate estimates of protein volume in a number of publications [164–168]. However, the model fails when heterogeneous distribution of ions results from electrostatic interactions with the surface of the pore and translocating particle [126,169].

If the nanopore volume is sufficiently large to allow the free rotation of non-spherical particles, the resistive pulse signature will depend not only on its volume, but also on its shape and relative orientation to the electric field [170]. There are several theoretical models to describe the pulse signal generated due to particle shape [171,172] under varying pore dimensions, surface charge, and electrolyte concentrations. Of these, the findings of Golibersuch [173], Fricke [174], Berge e*t al.* [175], Ito *et al.* [162], and Holden *et al.* [176] stand out in their use and extension of resistive pulse sensing for characterizing particulate samples. Golibersuch [173] and Berge *et al.* [175] have modelled and experimentally measured the difference in pulse signal arising from oblate (disc) and prolate (ellipsoid) particles.

Mayer's group took advantage of this model to approximate the shape of various individual proteins translocating through a nanopore [138,177]. It proposes a generalization of Maxwell's derivation.

$$\frac{\Delta I}{I_0} = \frac{\gamma\Lambda}{\pi r_p^2(l_p+1.6r_p)} S\left(\frac{r_p}{2R_h}\right) \qquad (6)$$

where Λ is the volume of the protein (m^3). γ is a form factor equal to 1.5 for a spherical geometry (Figure 3c), r_p is the nanopore radius and R_h is the hydrodynamic radius of the

protein. In the case of the spheroid, γ can take two values: $\gamma_{\parallel} = \frac{1}{1-n_{\parallel}}$ and $\gamma_{\perp} = \frac{1}{1-n_{\perp}}$ depending on the orientation of the protein (Figure 3d-e). Typically for an oblate spheroid with $m = a/b < 1$ is $n_{\parallel} = \frac{1}{1-m^2}\left[1 - \frac{m}{\sqrt{1-m^2}}\cos^{-1}(m)\right]$ and for a prolate spheroid with $m = a/b > 1$ $n_{\parallel} = \frac{1}{m^2-1}\left[\frac{m}{\sqrt{m^2-1}}\ln\left(m + \sqrt{m^2-1}\right) - 1\right]$ and $n_{\perp} = \frac{(1-n_{\parallel})}{2}$. Finally, $S\frac{r_p}{2R_h}$ is a correction factor.

$$S\frac{r_p}{2R_h} = \frac{1}{1-0.8\left({R_h}/{r_p}\right)^3} \qquad (7)$$

Furthermore, they propose an estimation of the net dipole moment of the pico-to nanomolar concentrations of proteins [178]. In contrast, the standard method for measuring the dipole moment, dielectric impedance spectroscopy, requires micromolar protein concentrations and significantly larger sample volumes. They measured simultaneously, these five parameters—size, charge, rotational diffusion coefficient, and dipole moment of individual proteins in aqueous solution under nondenaturing conditions [177]. They found that the most probable speed at which the particle transit between these orientations is proportional to its bulk rotational diffusion coefficient.

The approach based only on volume exclusion and ohmic consideration is generally not suitable for asymmetric nanopores with high aspect ratio due to a non-homogeneous ionic distribution along the nanopore. Nevertheless, in the specific case of conical nanopore coated with uncharged function, a 1D model based on the sum of resistance can be applied to correlates the relative current blockade to the size of a cylinder Eq 8 (Figure 3f) [151]. This model was applied in the case of amyloid fibrils with a radius r_{amy} and length L_{amy}

$$R_{max} = \frac{1}{G_{min}} = \frac{1}{\kappa\pi}\left[\frac{1}{2ar_{amy}}\log\left(\frac{(aL_{amy}+r_t-r_{amy})(r_t+r_{amy})}{(aL_{amy}+r_t+r_{amy})(r_t-r_{amy})}\right) + \frac{L_p-L_{amy}}{(r_t+aL_{amy})r_B}\right] \qquad (8)$$

Where maximum resistance R_{max}, L_p r_t and r_B are the nanopore length, the tip and the base radii respectively. However, this model assumes that the fibril is perfectly aligned inside the nanopore. In addition, it is suitable only when the tip size is close to the fibril diameter. Conversely to the relative current blockade, there is a huge discrepancy between the estimated and measured dwell time and capture rate that is important to discuss [139,140]. The capture rate and the dwell time involve many phenomena including the interaction with the surface, electroosmotic flow, etc. At first approximation, the dwell time Δt of a globular and rigid protein can be written as [168].

$$\Delta t = \frac{C_f \eta l_{eff}^2}{QV} \qquad (8)$$

where $\eta$is the solution viscosity, C_f is a constant for a protein shape, l_{eff} is the effective length of nanopore, Q is the total charge of protein and V is the bias potential. A simple calculation of the expected dwell time for a globular protein such as BSA gives a result several orders of magnitude smaller than the recorded one [168]. Typically, the translocation of sub-100 kDa protein molecules through solid-state nanopores with diameters ~10 nm, is expected at μs scale but only the slowest 0.1% of the translocations are observed when using current amplifiers with 10 kHz bandwidth [140,179]. In literature, the reported dwell time is often two or three orders of magnitude longer [154,157,180]. Plesa *et al.* investigated the limitations on protein detection as a function of their size assuming the absence of specific interactions. They successfully detected aprotinin, ovalbumin, β-amylase, ferritin , and thyroglobulin using silicon nitride nanopore with the diameter of 40 nm [140]. They compared the experimental dwell time with the electrophoresis mobility μ predicted with the Einstein-Smoluchowski relation, according to 1D first-passage time-distribution model.

$$\mu(r) = \frac{D(r)}{k_B T} \quad (9)$$

Where *r* is the nanopore radius, *D* is the diffusion coefficient of the protein n, K_b is the Boltzmann constant and *T* is the temperature in Kelvin. The diffusion coefficient of the proteins depends on their molecular weight and their geometrical features. They found a distortion of the measured current because the proteins translocate too fast through the nanopore. Besides the dwell time, the capture rate is also different from the expected one. It can be estimated assuming that the diffusion governs the protein motion until a region in the vicinity of the nanopore (r_p*) [181].

$$f_d = 2\pi c D r_p \quad (10)$$

where *c* and *D* are the concentration and the diffusion coefficient of the protein respectively. In the case of non-deformable nanoparticles that do not interact with the nanopore surface, the estimated capture rate fit well with the experimental data [182]. In the case of protein, the capture rate is lower by several orders of magnitude [139,140,183]. There are different parameters that can explain the long dwell time and the low capture rate. Plesa *et al.* calculated the event loss ratio as a function of the drift velocity of the proteins and the diffusion coefficient [140]. They revealed that application of the 10 kHz low pass Bessel filter caused a severe loss of the translocation signals for proteins with molecular weight <50 kDa because of the temporal resolution limit, suggesting that an amplifier with a higher data acquisition frequency is required for protein detection. Balme *et al.* reported a correlation between the protein adsorption and the capture rate of several proteins [139]. They suggested that only the proteins that transiently interact with the nanopore inner surface could be detected using amplifier with a sampling rate 200 kHz and

filter 10 kHz. The role of protein adsorption was also suggested by Sexton *et al*. in the case of PET nanopore [184].

4.1.1.1. Adsorption

One issue of the protein sensing using solid-state nanopore is the nonspecific adsorption that is difficult to predict [185]. Even if, the adsorption allows to slowdown protein translocation, it can generate a modification of nanopore surface state and diameter until its clogging [138]. The SiN is hydrophobic and under nanopore experience condition (ionic strength and protein concentration), the interfacial concentration at the equilibrium is low reaching thousands of proteins/μm^2 [139]. The classical methods of preparation of SiN chips consist to oxidase the surface by piranha, ozone or oxygen plasma. This ensures a clean and hydrophilic surface, and thus, significantly decreases the protein adsorption. To optimize the antifouling properties, the nanopore can be functionalized. The PEG grafting directly by silanization reaction was found to efficiently prevent the adsorption of protein aggregates [143]. This strategy also presents the advantage to significantly improve the nanopore lifetime [186]. The PEG grafting was also used in the with PET nanopore [151]. The PEG can also be deposited by self-assembly chemistry after the deposition of gold layer [187]. The performance of PEG to prevent the protein adsorption is dependent on its conformation and surface density and thus have the effect of the interaction between PEG and the nanopore surface well taken into account [188].

The physisorption of the surfactant such as Tween 20 was also considered to prevent the adsorption of α-synuclein [189]. The SiN pore walls coated with a fluid lipid bilayer providing, on the one hand, a non-sticking, non-fouling surface and, on the other hand, capture protein anchoring on lipid allowing slowing down [138,190]. The lipid coating was

also reported on glass nanopipette [191]. More recently, several zwiterionic polymers were considered for SiN nanopore coating [192].

4.1.1.2. How to detect each event during protein translocation?

The first way to improve the protein detection is to slow down their motion to increase their dwell time within the nanopore until a time-resolvable signal. Because the protein charge is involved in the dwell time, one solution is to work at pH close to the isoelectric point of the protein [180]. In that case, translocation of the protein can be slowed down because of the diminished electrophoretic mobility when the net charge of the protein molecules approaches zero [193]. This leads to longer residence time improving the temporal resolution. The decreased translocation speed enabled detection of ubiquitin (Ub). In addition, two Ub dimers with the same molecular weight, but different molecular structures, were readily discriminated [193]. Furthermore, the authors used the method to monitor deubiquitination reactions of di-Ub. An alternative approach toward improving the statistics based on one protein traversing the nanopore is to control the capture rate. The influence of electroosmotic flow has also been considered for artificial but also biological nanopore [194]. The SiNx nanopore has a slight negative charge at certain pH or under light. This induces a cation-based electroosmotic flow that can further slowdown the protein translocation [180,195–197]. Another strategy is to bind protein with a ligand inside nanopore [165]. The use of a carrier to drive the protein can also be a solution. The DNA carrier strands containing an aptamer sequence were bound to specific target proteins [198–200]. The protein detection was provided by the analysis of sub peaks corresponding to the protein in the ionic current blockade when DNA strands translocated through the

pore. Such approach takes the advantage to specifically detect a protein target from serum protein but also the specific interaction protein DNA like DNA-repair protein RecA [201]. The second way involves working directly on the signal. Achieving the higher signal-to-noise ratio with classical amplifiers (frequency 250 kHz) required that a protein resides in the nanopore's sensing region for > 20 μs. However, 10 to 100 kHz acquisition bandwidths (defined by the application of a low-pass filter) have often been used in nanopore sensing despite capturing only a fraction of the events. To reach the detection of events with dwell time about 1 μs the system bandwidth should be in MHz scale. In practice, the temporal resolution in nanopore sensing is given by the RMS:

$$SNR = \frac{(\Delta I/I_0)}{I_{RMS}} \quad (11)$$

where I_{RMS} is the noise approximated by the root-mean-square (RMS) of I_0. For example, an SNR ratio of 5 is obtained, with a signal amplitude of 0.5 nA and an associated root-mean-square (I_{RMS}) noise of 0.1 nA, measured at a bandwidth of 100 kHz. When this RMS is smaller than 2 sensing might become impractical since the translocation events cannot be differentiated from the background noise [140]. The RMS noise is composed by different terms expressed as following

$$I_{RMS}^2 = \int Sdf = I_{Flicker}^2 \propto (\ln(f)) + I_{Thermal}^2 \propto (f/R_P) + I_{Dielectric}^2 \propto (f^2) + I_{Amp}^2 \propto (f^3) \quad (12)$$

where S is the noise powers from the different sources $S_{Flicker}$, $S_{Thermal}$, $S_{Dielectric}$, and S_{Amp}, f is the sampling frequency, and R_P is the pore resistance [34,202–204]. $S_{Flicker}$ and $S_{Thermal}$ are all related to the ionic current level through the nanopore. $S_{Flicker}$ is also dependent on the membrane material. The thermal noise is less pronounced than the other sources in typical nanopore measurements [204]. On the contrary, dielectric and amplifier noises are

significantly affected by the properties of the substrate material. To date, a variety of approaches has been proposed to increase signal-to-noise ratio. The SiN nanopore can be passivated by Al_2O_3 to improve the signal noise ratio (SNR) [205,206]. Such coating also allows to improve the signal in the case of PET nanopore [207]. Glass nanopipette provides low electrical noise showing root-mean-square (RMS) of 2.4 pA at 10 kHz bandwidth. It has been used for the detection of a wide range of protein molecules weight from 14 kDa to 465 kDa including lysozyme, avidin, and IgG [208]. The curing of PDMS on the nanopore ship reduce the I_{RMS} by a factor 5 [209,210]. The use of several substrates such as quartz allows reducing the dielectric noise about one order of magnitude [211]. A detailed benchmark for the noise a function of nanopore material was previously reported [34].

Improved electronics capable of measurements with bandwidth as quick as 1 MHz is another strategy to reach a temporal resolution of 1 μs [212]. Larkin *et al.* employed a high bandwidth amplifier sampling the ionic current signals at a 4 MHz frequency and filtering the high-frequency signals at 250 kHz (Figure 4a) [181]. They concluded that with the signal amplifier having the MHz bandwidth, 30–80% of the events were detected among RNase translocation events, and 70–90% of the events were detected among proteinase K translocations. They also propose a 1D drift-diffusion model that assumes barrier-free transport to fit protein translocation dwell-time distributions:

$$P(t) = (h_{eff}/4\pi D_{pore} t^3)^{1/2} e^{-(h_{eff} - v_d t)^2 / 4 D_{pore} t} \qquad (13)$$

Where h_{eff} is the effective pore thickness, D_{pore} is the diffusion coefficient of protein through the pore, and v_d is the protein drift velocity inside the pore.

Accordingly, to improve the resolution of proteins sensing in the solid-state nanopore, it is necessary to use a high-frequency amplifier and a nanopore device with low electrical noise. The detection of protein molecules through nanopores in SiNx and HfO_2 nanopore have been performed by high-bandwidth (1 MHz) electrical measurements. It allowed the direct discrimination of ubiquitin and ubiquitin chain [193], the investigation of protein flexibility [213], as well as conformational change [141,214]. Such electronic device has already shown promise in a variety of exciting applications for protein sensing.

Recently, new simple ways were proposed to increase resolution: the crowded media. The strategy proposes to add polymers in the nanopore system to create a crowding environment; this media allows to slowdown the translocation speed of the protein and increase the current perturbation. Originally, this approach was used to improve the detection of DNA samples [195,215–217] . Schmidt *et al.* investigate the BSA and IgG present in solution thanks to the molecular crowding effect. They added PEG DMA 1 kDa on the cis side of the pore and observed an increase in the frequency events as well as in the dwell time. This approach allowed the discrimination of BSA and IgG based on the amplitude of the current blockade [218]. Recently, Actis et *al*. added PEG 8 kDa (or 4 kDa) at different percentage of weight/volume on the trans-side of a glass nanopipette. They report an increase of events rate, dwell time and current blockade amplitude for the β-galactosidase (Figure 4b). They were able to observe differences between elongated fibrils and fragmented fibrils of α-synuclein thanks to the improvement of sensibility due to the presence of PEG [219]. Overall, the molecular crowding allows an increase in the sensitivity of the nanopore. The main advantage is their simplicity to set up. Indeed, it consists just to add polymers on a specific side (or both) allowing the slowdown of the

translocating analyte as well as an increase in current peak amplitude and frequency. Al Sulaiman et *al*. functionalized the nanopipette by grafting polymers. The hydrogel slowdown of DNA translocation allowing the detection of fragments as small as 100 bp using a nanopore with a diameter of 20 nm [220]. However, the crowding arises several questions relative to the location of the polymer inside the nanopore and its impact on the recorded current blockade amplitude. Several models allow linking the current blockade to the protein volume and shaping as soon as the experiments are conducted in saline solution. Using crowding, such model becomes wrong and thus new ones should be developed. This involves deeply understanding the role and the location of the polymer.

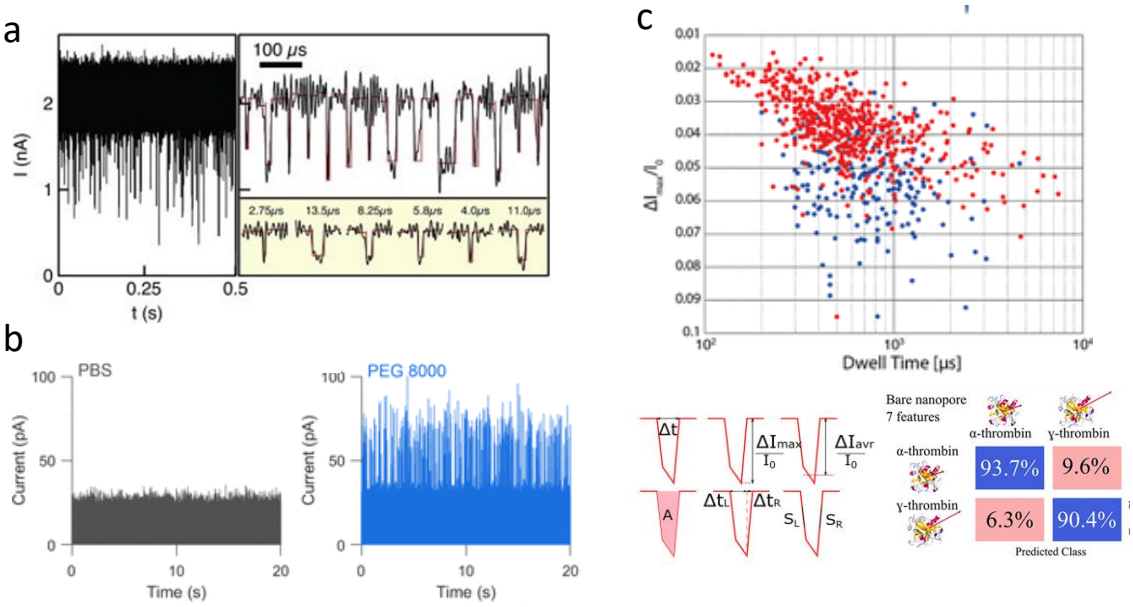

Figure 4 : (a) Current trace for proteinase K detection by HfO_2 nanopore recorded using Chimera data sampled at 4.19 MHz and digitally low-pass-filtered at 250 kHz, Reproduced with permission [181], 2014, Elseiver.(b) Current trace induced by β-galactosidase through glass nanopipette in PBS (left, black) and PBS with 50% (w/v) PEG 8000 kDa (right, blue), Reproduced with permission [219], 2020, American Chemical Society. (c) top, Event map of γ-thrombin and α-thrombin (blue and red respectively) obtained with a SiN nanopore. Bottom, left, features (parameters) of resistive pulse events used for protein discrimination using machine learning. Bottom, right, confusion matrices for seven features showing the capabilities for prediction and classification of γ-thrombin and α-thrombin in the bare nanopore, Reproduced with permission [221], 2021, American Chemical Society.

4.1.2. Improve the nanopore resolution using machine learning

The machine learning is an interesting strategy to improve the object discrimination by nanopore sensing. It has been used for a long time for DNA analysis using biological nanopore [222,223]. In the case of solid-state nanopore, the use of machine learning grew up recently. However, such approach requires considering the events with more than the two usual parameters (dwell time and relative current blockade). Several strategies were reported, the consideration of additional current blockade parameters such as the slope, the integral, etc [224]. The main idea is to find additional patterns in the signal that can be attributed to the analyte. In terms of methodology, the classical clustering classification as well as neuronal networks were considered [225]. Generally speaking, regardless the machine learning methodology, the discrimination of the analyte is improved as shown for the short DNA [224] , glycosaminoglycan [226,227] and virus [147,228–230]. The machine learning was also used to discriminate α- and γ-thrombin with interesting accuracy since the positive predictive values reach 96.5% while the events map plotting the amplitude and the dwell time of current blockades are strongly overlapping (Figure 4c) [221].

4.2. Applications on protein sensing

4.2.1. Peptide sensing

Compared to the biological nanopore that is well adapted to peptide sensing, the artificial nanopore is not a suitable candidate. The main difficulty to detect polypeptide through solid-state nanopore is the relative short dwell time. This requires using ultrafast amplifier with low noise level, or to find a way to slow down the peptide. The first strategy is used to determine the cysteine position of a polypeptide of 41 amino acids [231]. Another way is to increase the dwell time using nanopore with high aspect ratio. This strategy was

suitable for poly-L-lysine with molecular weight greater than 4 kDa since the resolution of such nanopore is very low. The deposition of PLL inside a conical PET nanopore induces an inversion of current rectification. [94]. This was also reported inside a quartz nanopipette [232].

4.2.2. Identification of protein

As previously discussed, the nanopore resistive pulse technique allows assigning the current parameter to a protein. The avidin was considered as a model to investigate the effect of electrophoretic and electroosmotic flow on the detection through SiN nanopore. [180] Plesa *et al.* investigated the limitations on protein detection as a function of their size assuming the absence of specific interactions. Using nanopore with a diameter 40 the range of protein includes aprotinin (6.5 kDa), ovalbumin (6.5 kDa), β-amylase (45 kDa), ferritin (200 kDa), and thyroglobulin (660 kDa) [140]. Fologea *et al.* discriminated the BSA and the fibrinogen based on the difference of the current blockade and the dwell time (Figure 5a) [168]. However, the distribution of amplitude of the current blockade can show large overlap if the size of the proteins are too similar as reported for BSA, ovalbumin and strepavidin [161]. Because protein discrimination is impossible if their size is too close, SiN functionalizations to obtain a specific interaction with the target protein were developed [233]. Fanzion *et al.* functionalized SiN nanopore with Locked Nucleic Acid to specifically interact with the Nuclear Factor-kappa B proteins. The functionalization allows the specific detection of P50 protein. Interestingly, the distribution of current perturbation value suggests several occupancy state of the nanopore [234]. Wei *et al.* grafted nitrilotriacetic acid inside SiN nanopore to specifically detect protein with His-tag [165]. Such functionalization involves a gold layer deposition prior PEG self-assembly.

The nanopore was used to detect specifically IgG. However, the pore were unable to differentiate the different types of IgG. The discrimination of two close proteins using SiN nanopore is highly challenging. It was demonstrated that the combination of aptamer functionalization and machine learning approach could significantly improve the discrimination of a- and y- thrombin [112]. This way underlines the interest to functionalize SiN nanopore with ligands that are specific to protein such as avidin-biotin [235] system or NTA his-tag [165] to increase the dwell time of the interest protein.

The approach involving lipid bilayer coating combined to the detection of anchored protein to the lipid is up to now the most efficient. as it allowed to differentiate proteins from their size, shape and dipolar moment [178]. Using that Mayer's group have correlated the current blockade distribution with the geometry of ten proteins including BSA, streptavidin, IgG, GPI-AChE, G6PDH, β-PE, BChE, α-amylase, i-LHD and Fab. Such investigation involves that the lipid coating must be perfectly controlled to correctly assign the protein shape and translocation signal. Indeed, the composition of the coating influences the baseline stability, the noise level, the translocation speed [190]. From the theoretical point of view, the protein properties could be extracted from the current perturbations if they freely translocate through the nanopore. This point is of critical importance. Indeed, it involves preventing the protein adsorption inside the nanopore by developing anti-adhesive approaches, but also to use a high-speed amplifier with a reasonable noise [178].

The protein adsorption on nanoparticles is strongly dependent on their structure. The nanopore sensing is a suitable technique to investigate the stability of protein- nanoparticles interaction. Coglitore *et al.* investigated the protein corona on gold nanoparticles using SiN nanopore. They showed that the volume of the first layer of proteins is driven by their

structural categories (mainly α-helix, mainly β-sheets or a mix-α-helix and β-sheet) and thus their internal energy [149]. They also demonstrated that the resveratrol binding changes the BSA adsorption onto the gold nanoparticles making it reversible [148].

The protein detection by polymer nanopore was performed using the resistive pulse method. The conical nanopore obtained with the electrostopping method allow controlling the tip aperture until reaching a size compatible for protein detection [236]. As for SiN nanopore the functionalization to prevent the protein adsorption is required. There are two strategies. The first one consists to deposit gold by electroless deposition and SH-PEG coating. The second one is the direct grafting of NH_2-PEG on COOH moieties presents on the pore walls. Using such nanopore, several proteins were detected such as BSA [237], phosphorylase B, and β-galactosidase [184]. The PET conical nanopore was also efficient to detect protein/antibody complex such as BSA vs. anti-BSA-Fab [238]. BSA was also detected using a conical PET nanopore coated with Al_2O_3 by atomic layer deposition. Both techniques reduced the pore size closer to the protein. The interaction of the BSA with the surface slows down the transport of the protein through the pore via sorption/desorption process on the Al_2O_3 surface [239]. The main issue of the track-etched nanopore is their low resolution and low current level that make impossible the protein discrimination. This is a reason why they are less considered than solid-state nanopore. However, they offer several advantages. Their tunable geometry and the presence of COOH moieties allow easy functionalization of the nanopore.

The nanopipettes were also considered to detect proteins. Keyser's group used nanopipette to detect lysozyme, avidin, IgG, β-lactoglobulin, ovalbumin, BSA and β-galactosidase. For SiN pores, the authors did not establish if the events are ballistic or involve transient

adsorption. [208] Conversely, proteins with wide molecular weight range can be discriminated using nanopipette. This was demonstrated for a protein range from 12 kDa to 480 kDa (GFP, RNA polymerase, FP, IgG) [240]. To improve the nanopipette selectivity, Ying *et al.* functionalized a nanopipette with an antibody and then specifically detected the antigen. This strategy also allows the characterization of protein-protein interactions at single molecule level [241].

Farimani *et al.* were able to distinguish between different subclasses of antibodies using a 2D graphene nanopore. First, they simulated different IgG antibody subclasses (IgG2 and IgG3) entering the nanopores. The antibody subclasses have a 95% similar structure and are only different at the hinge region. From this simulation, they concluded that they could differentiate several antibody subclasses by ionic current if enough translocation events were available. This simulation was then followed by using machine learning to detect these events after measuring the ionic current, the dwell time, and the water flux for the translocation of each subclass. Finally, they compared the results of using a 2D graphene nanopore with a silicon nitride nanopore and found that the silicon nitride pore cannot distinguish between different IgG subclasses [242].

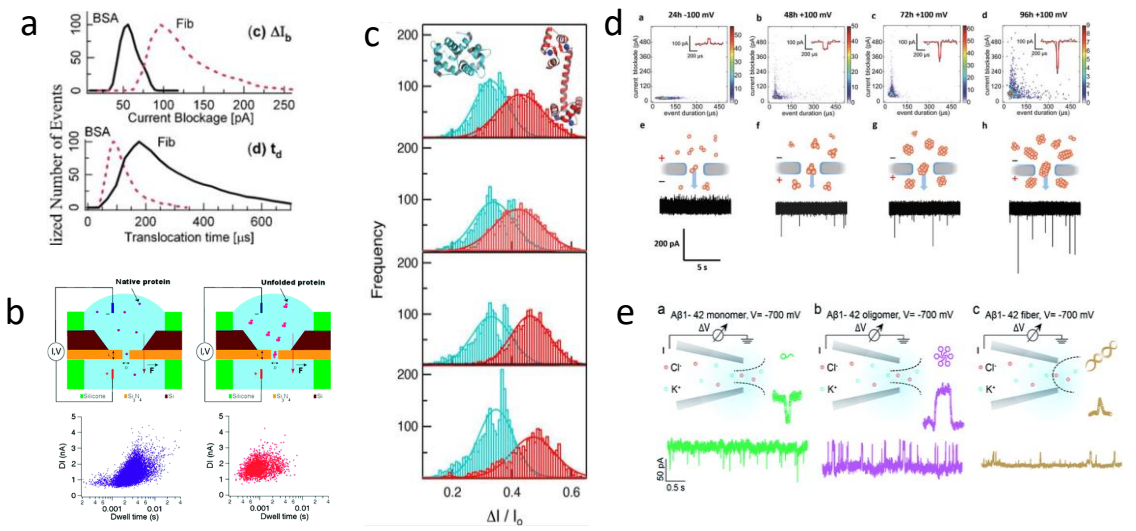

Figure 5: (a) detection of BSA and fibrinogen using SiN nanopore distribution histogram of the current blockade (top) and dwell time (bottom) Reproduced with permission [168], 2007, AIP publishing. (b) scatter plot of events recorded for MBP proteins folded (left) and unfolded (right), Reproduced with permission [154], 2011, American Chemical Society. (c) distribution histogram of the current blockade at various voltage for the calmodulin with (blue) and without (red) loaded calcium obtained with SiN nanopore, Reproduced with permission [141], 2017, American Chemical Society. (d) Kinetic of α-synuclein aggregation evidenced by SiN nanopore coated with tween 20. the subpanels a,c,b,d represent the event map for various incubation time of α-synuclein from 24h to 96 h. subpanels e,f,g,h, illustrated the oligomer size that translocates through the nanopore and a current trace recorded, Reproduced with permission [189], 2016, Springer Nature. (e) detection of different Aβ42 aggregate structure using nanopipette. Subpanels a,b,c are illustration of the Aβ42 detection using nanopipette and an example of current trace at various aggregation stage : monomer, oligomers and fibres respectively, Nature Publishing Group [127], 2019, Royal Society of Chemistry.

4.2.3. Conformational change

The 3D structure of a protein confers to them their properties. Some small changes are often at the origin of physiological troubles. Because the protein shape can be correlated to the current perturbation, the resistive pulse technique is a promising way to investigate protein conformational changes. In this field, the first works aim to investigate the protein unfolding process. Indeed, the modification of the volume and diffusion coefficient of unfolded proteins can be identified by a shift of both the current blockade and dwell time (Figure 5b) [154,243]. Varongchayakul *et al.* investigated the conformational change for different vascular endothelial growth factor receptor (VEGFR) isoforms caused by slight variations of pH. They found that below the pI of VEGFR (pH=7.2), it loses its native structure, exposing positive charged domain to its surface. The loss of structure was also

confirmed by the lack of specific antibody binding [170]. To study the effects of drugs on the conformational change of proteins, Hongsik Chae *et al.* created a fusion protein of murine double minute 2 (MDM2) linked to a p53 transactivation domain using a 16 amino acid long linker ((GGGS)4). This fusion protein contains a large glutathione-S-transferase at the C-terminus. In this work, solid-state nanopore was used to successfully detect the conformational change of the fusion protein induced by the presence of nutelin-3 [214].

In another study, Hu *et al.* used a solid-state nanopore to detect and characterize the conformational changes of enzymes that resulted from the binding of their respective substrates. The first measurements were carried out by studying the effect of the binding of diadenosine pentaphosphate to adenylate kinases. The binding of the substrate leads to a loss in the enzyme flexibility that was characterized by the reduction in the full width at half maximum (FWHM) of the ion current signal distributions between the unbound and bound kinase. The conformational changes were investigated between the wild-type dihydrofolate reductase and different mutants with known conformational flexibility. The experiment consisted of measuring the different conformational flexibility changes that occur with each mutation. The resulting measurements were correlated with the bis-ANS fluorescence technique proving the validity of using nanopores for the measurements of conformational flexibility [213]. Laura Restrepo-Pérez *et al.* simulated the translocation of proteins through a 6.5 nm SiN nanopore assisted by SDS. The simulation included a protein monomer, a dimer and β-amyloids. The results suggest that translocation of proteins through SDS can be used to identify the proteins by their translocation time. In addition, the simulation reveal that the proteins are translocated through electrophoretic forces due to the enhanced negative charge of the SDS, which coats the entirety of the protein. The

experimental results show that the SDS reverse the direction of the translocation as indicated in the simulation. However, the decrease of the amplitude of the current blockade dramatically alters the process of protein translocation through the solid-state nanopore [244]. Waduge *et al.* used a silicon nitride and hafnium oxide pore to study the transport of proteins in their native state. They used the electroosmotic forces to capture the proteins at subpicomolar levels efficiently. First, they experimentally determined the radii of the protein, which correlates with their calculated gyration from PDB coordinates. This was followed by the investigation of the structural flexibility of the proteins by measuring the FWHM of current amplitude distribution and the RMSF values from the structure-based simulations. They found a significant change in the dwell time and current blockage statistics between the calcium-free calmodulin and the calcium loaded calmodulin, suggesting a change in the flexibility between each state (Figure 5c) [141]. The conformational change of the protein can occur during the translocation process due to the applied voltage. This was reported for the human serum transferrin protein through 2D hexagonal boron nitride at 400 mV [245].

4.2.4. Protein assembly

The resistive pulse provides information on the residence time of the analyte inside the nanopore. This allows the characterization of the protein assembly with a probe attached onto the nanopore inner wall. This strategy follows the one developed for biosensors [246]. Yanfang Wu e*t al.* reported the development of a nanopore biosensor for the detection of prostate serum antigen (PSA). First, the silicon nitride based conic nanopores was coated with gold using vapour deposition. The gold surface of the pores was then functionalized using thiolization using alkenothioles, which allows the deposition of -COOH, groups on

the surface of the pores. EDC\NHS was then used to graft anti-PSA antibodies. A secondary anti-PSA antibody was then immobilized on magnetic nanoparticles. The detection occurred when PSA formed a sandwich assay between the magnetic nanoparticles and the nanopores. This assembly blocks the nanopores. Indeed, when a reverse magnetic field was applied the unbound MNP exit from the nanopores the presence of PSA by current blockade [247].

Das *et al.* developed a biosensor for the detection of thrombin using a quartz nanopipette. They functionalize the nanopiette with a 5' amino-modified thrombin aptamer with a six-carbon spacer (5'-AmM-C6-GGTTGGTGTGGTTGG-3'). Then, protein concentrations were measured using the intensity blockade of the ionic current of the electrolyte-filled nanopore. The signal was processed using the Monte Carlo simulation. The resulting biosensor was suitable to detect the thrombin in human serum for a concentration down to 50 pM with a response time of 10 min [248]. Yi-Lun Ying *et al.* developed a functionalized nanopipette for the detection of α-fetal protein (AFP). A gold layer was deposited then a single antibody was immobilized. The translocation of AFP through the nanopore reveals a tenfold increase in dwell time after the functionalization. This also allows a monitoring of the antibody/antigen binding in real time [241].

4.2.5. Protein aggregates

The protein aggregation is involved in numerous pathologies including Alzheimer's disease and Parkinson's disease. The solid-state nanopore was considered as a single molecule sensor to provide information on protein oligomerization and aggregation. Like for proteins, silicon-based, nanopipette and track-etched nanopores were considered to detect and attempt to characterize protein aggregates. Using SiN the oligomer of lysozyme were

discriminated [143]. However, the adsorption of the protein aggregates on the inner walls of the pore leads to fouling of the pore. To prevent that, the chemical grafting of PEG was considered. Using this strategy, it was possible to discriminate ordered aggregates lysozyme and beta-lactoglobulin from amorphous albumin based on the different shapes of current blockades [139].

Intrinsically disordered proteins such as Aβ, α-synuclein or tau are known for their tendency to adsorb on surfaces inducing pore clogging. Yusko *et al.* used a lipid coating to reduce the interaction between Aβ and the SiN nanopore. Their approaches allowed them to significantly reduce adsorption and thus detect Aβ1-40 aggregates [138]. The amplitudes of the current blockade are correlated to the geometric parameters of the assembly thanks to Maxwell's derivation model [143]. Consequently by analysis of the amplitude of the current blockade and the dwell time, it is possible to discriminate different amyloid assemblies [142]. For the detection of α-synuclein, the SiN nanopore was coated with tween 20. Using such nanopore Hu and coworker follow the α-synuclein aggregation during 24 h [189]. Interestingly, the translocation of small oligomers or monomer induced a current enhancement interpreted by the high number of charges of the protein (Figure 5d).

Very recently, SiN nanopore have been used to follow the aggregation of α-synuclein and two of its mutants known to be pro aggregative. The resolution of the pore does not allow detecting monomers and too large fibres. Only the oligomers and small protofibers were observed after 6 days for the two mutants whereas for WT it was after 10 days. This confirms the pro-aggregative nature of the two mutants compared to WT [249]. This paper highlights a problem of SiN nanopore. Indeed, to observe protofibrils or fibrils, the

nanopore diameter has to be large enough to allow their translocation leading to a lower resolution for oligomers of smaller size. Conversely, to detect monomers and oligomers, the nanopore diameter should be smaller but then larger assemblies like fibrils tend to clog the pore.

The glass nanopipettes are also suitable to investigate amyloid assemblies. U. Keyser and his collaborators have successfully detected prion aggregates. An interesting fact is that they have not reported any phenomenon of clogging with their experimental conditions [208]. The same group have then followed the aggregation of lysozyme. They were able to identify different intermediates without the problem of clogging [250]. A recent paper shows detection of different amyloid assemblies of Aβ-42 peptides by glass nanopipette. This work highlights different types of events depending on the aggregation time (Figure 5e). While monomers induce a current enhancement, oligomers translocate through the nanopore inducing a blockade with a long dwell time likely due to a transient interaction amyloid/nanopore. Finally, the fibrils are characterized by bumping events. This paper also shows a very significant adsorption of the Aβ-42 oligomers compared to the other species. This property can be an explanation of their highly neurotoxic feature [127]. The common point of these studies is that the protein aggregate was placed outside the nanopipette. Thus, the problem that the fibre cannot enter inside the nanopore pointed out previously for the SiN is the same. More recently, Chau e*t al.* placed α-synuclein fibres inside the nanopipette allowing their detection as well as the small aggregate obtained by sonication [219].

An alternative to detect small oligomers and fibrils in a same nanopore was to use track-etched nanopore with conical shape. Indeed, the large aperture (>200 nm) allows capturing large assemblies and the small aperture allow the detection with good resolution. Solid-

state nanopore coated with PEG is required to prevent the fouling. Using this strategy, the kinetic of β-lactoglobulin was followed showing different aggregated population, i.e., oligomers and protofibrils. Another advantage of the track-etched nanopore is their long lifetime since one nanopore can be utilized several weeks [151]. The same group investigated the aggregation of Tau induced by heparin. They evidence an enhancement of aggregation for the P301L mutant compared to the wild-type. Interestingly, the fluctuations observed during long translocation events were interpreted by and increased flexibility of the mutant as well as a greater capacity for fragmentation [251].

4.2.6. Probing enzymatic reaction by resistive pulse sensing

The enzymatic reaction was investigated by resistive pulse technique following two approaches. In the first one, the nanopore serves to analyse the product of the enzymatic reaction. This approach was reported by Giamblanco et *al*. to investigate the enzymatic degradation of β-lactoglobulin amyloid by trypsin and pepsin using track-etched nanopore. This work highlighted that a reaggregation process occurs for the enzymatic degradation by pepsin at pH 2 due to the autodegradation of the enzyme. Conversely, no reaggregation occurred with trypsin at pH 9 [252] suggesting that the amyloid digestion has different kinetics and released products between the gastric digestion and the intestine.

In the second approach, the enzyme is grafted inside the nanopore making possible to determine a characteristic time of the enzymatic reaction. Considering a conical nanopore with high aspect ratio, the hyaluronidase was grafted close to the large entrance of the nanopore. In that case, it becomes possible to detect the product of enzymatic reaction. More interesting, when the enzyme is grafted close to the small entrance, the characteristic time of enzyme substrate can be observed [253].

5. Conclusion and outlook

To sum up, solid-state and polymer nanopores can serve in numerous applications in protein sensing, however, compared to the biological ones, they are not in the centre of commercial applications. To achieve that, several bottlenecks must be tackled in the next years. The main limitation of solid-state and polymer nanopores comes from the difficulty to control their size, shape and surface state precisely. For the SiN, it is important to notice the difficulty of filling the pore with aqueous solutions even if piranha treatment, ozone or O_2 plasma increase the surface wettability. In addition, the conversion of SiN to SiOH due to the oxidation increases the surface energy of the nanopore surface. As this system evolves to decrease its global energy, there is a decrease in wetting due to interactions with the impurities present in the buffer leading to a reduction in the duration of use. The dielectric breakdown is an alternative to the filling problem; however, the inner surface of the nanopore is not perfectly controlled. Another important problem is the nanopore lifetime due to the modification of the SiN surface state during the experiment. Nanopipettes are an interesting alternative to the SiN since they can also be functionalized and can be easily filled by process involving distillation and condensation using tantalum filaments or a simple hot plate as a heater. [254,255]. For SiN and nanopipette, a controlled functionalization using hydrophilic and anti-adhesive functionalization is required to prevent the fouling. As an example, the PEG allows improving the SiN nanopore lifetime. Here, it is important to note that ideally the functionalization should be done in aqueous solution or in water miscible solvent. Track-etched nanopores could be ideal since it is filled directly after the aperture and the functionalization with hydrophilic molecules can be done in water solvent. However, they suffer from two limitations. First, the resolution cannot allow to discriminate proteins. Indeed, only population of amyloids can be

differentiated due to the low resolution of the conical nanopore. The second problem is that it is impossible to produce two identical conical nanopores. This limits the application especially for the resistive pulse. However, the use of bullet-like shaped pores allows reducing the disparity of the nanopore size. Deep investigation to adjust the parameter of the etching condition is still required to better control the nanopore size. The second improvement consists to increase the resolution of artificial nanopores. Chemical functionalization can improve the sensitivity. However, functionalization steps are often complex, exhibit low yield and cannot allow a perfect control of the surface [219]. Indeed, the chemical grafting requires active moieties that are not homogenous along the nanopore and their density not totally controlled. One question that is often not clearly address is the measurement of the surface density of the molecule grafted inside a nanopore. Some raw estimation can be obtained from the volume reduction of the nanopore[235] . However, the exact grafting rate can be obtained for PET track-etched nanopore with high aspect ratio for those the exact surface charge can be deduced from analytical models[77,256] .

In order to obtain a homogenous surface and reproducible active moieties, the physical deposition after nanopore opening using atomic layer deposition could be a solution. However, such technique is difficult to control and provides a lot a fail. The crowded media could also be interesting alternative to the chemical functionalization. Nevertheless, several questions have to be solved such as the location of the polymer inside the nanopore and its impact on the recorded current blockade amplitude. Solving these questions will be crucial to develop models to assign the current perturbation parameter to the protein properties. The development of high speed and low noise amplifiers leads a better resolution of objects translocating providing very interesting results for the protein sensing [220]. Such

amplifier will become essential for the protein sensing with nanopore of low aspect ratio. Besides, the improvement of the experimental setup, the data treatment also requires further advances. Indeed, the description of the current perturbation by several additional parameters combined to machine learning seems a promising way for protein discrimination.

The most common used nanopore (SiN, polymer and nanopipette) does not offer a suitable resolution for protein sequencing. Indeed, the latter is one of the biggest challenges of protein sensing [257–259] . In this field, the biological nanopore (i.e., aerolysin [23,136], MSPA [21,22] and FraC [260]) combined or not to complex biomolecular process are suitable to identify one amino-acid on a peptide chain. However, in this field the 2D-nanopore could be an alternative as suggested by recent theoretical investigation using molecular dynamic simulation[261,262].

Despite existing limitations, solid-state nanopores have demonstrated their efficiency to analyse proteins. Indeed, they make possible to analyse their shape, flexibility conformational change, enzymatic reaction, protein-protein interaction and aggregation. Considering their great potentialities, nanopore sensing opens the way to numerous applications that offers the proteomic approach from the understanding of fundamental protein behaviour to personalized medicine. In this context, the future advances would probably be the identification of rare biomarkers as well as the early diagnosis of proteopathies.

Acknowledgments

This work was founded by Agence Nationale de la Recherche (ANR-19-CE42-0006, NanoOligo).

References

[1] Manzoni C, Kia DA, Vandrovcova J, Hardy J, Wood NW, Lewis PA, Ferrari R. Genome, transcriptome and proteome: the rise of omics data and their integration in biomedical sciences. Briefings in Bioinformatics 2018;19(2):286–302.

[2] Onuchic JN, Luthey-Schulten Z, Wolynes PG. Theory of protein folding: the energy landscape perspective. Annu Rev Phys Chem 1997;48:545–600.

[3] Jahn TR, Radford SE. The Yin and Yang of protein folding. FEBS J 2005;272(23):5962–70.

[4] Malhotra P, Udgaonkar JB. Tuning Cooperativity on the Free Energy Landscape of Protein Folding. Biochemistry 2015;54(22):3431–41.

[5] Mallamace F, Corsaro C, Mallamace D, Vasi S, Vasi C, Baglioni P, Buldyrev SV, Chen S-H, Stanley HE. Energy landscape in protein folding and unfolding. Proc Natl Acad Sci USA 2016;113(12):3159–63.

[6] Min D, Jefferson RE, Bowie JU, Yoon T-Y. Mapping the energy landscape for second-stage folding of a single membrane protein. Nat Chem Biol 2015;11(12):981–7.

[7] Neupane K, Manuel AP, Woodside MT. Protein folding trajectories can be described quantitatively by one-dimensional diffusion over measured energy landscapes. Nature Physics, 12(7), 700-703. Nature Phys 2016;12(7):700–3.

[8] Chiti F, Dobson CM. Protein Misfolding, Amyloid Formation, and Human Disease: A Summary of Progress Over the Last Decade. Annu Rev Biochem 2017;86:27–68.

[9] Morris AM, Watzky MA, Finke RG. Protein aggregation kinetics, mechanism, and curve-fitting: a review of the literature. Biochim Biophys Acta 2009;1794(3):375–97.

[10] Arosio P, Knowles TPJ, Linse S. On the lag phase in amyloid fibril formation. Phys Chem Chem Phys 2015;17(12):7606–18.

[11] Castello F, Paredes JM, Ruedas-Rama MJ, Martin M, Roldan M, Casares S, Orte A. Two-Step Amyloid Aggregation: Sequential Lag Phase Intermediates. Sci Rep 2017;7(1):40065.

[12] Arter WE, Levin A, Krainer G, Knowles TPJ. Microfluidic approaches for the analysis of protein-protein interactions in solution. Biophys Rev 2020:1–11.

[13] Abe H, Kuroki M, Imakiire T, Yamauchi Y, Yamada H, Arakawa F, Kuroki M. Preparation of recombinant MK-1/Ep-CAM and establishment of an ELISA system for determining soluble MK-1/Ep-CAM levels in sera of cancer patients. Journal of Immunological Methods 2002;270(2):227–33.

[14] Walther TC, Mann M. Mass spectrometry–based proteomics in cell biology. The Journal of Cell Biology 2010;190(4):491–500.

[15] Chen Y, Barkley MD. Toward Understanding Tryptophan Fluorescence in Proteins †. Biochemistry 1998;37(28):9976–82.

[16] Liu J, Choi M, Stanenas AG, Byrd AK, Raney KD, Cohan C, Bianco PR. Novel, fluorescent, SSB protein chimeras with broad utility. Protein Science 2011;20(6):1005–20.

[17]Maity B, Sheff D, Fisher RA. Immunostaining. In: Laboratory Methods in Cell Biology - Imaging, Vol. 113. Elsevier; 2013. p. 81–105.

[18]Kasianowicz JJ, Brandin E, Branton D, Deamer DW. Characterization of individual polynucleotide molecules using a membrane channel. Proc Natl Acad Sci USA 1996;93(24):13770–3.

[19]Jain M, Olsen HE, Paten B, Akeson M. The Oxford Nanopore MinION: delivery of nanopore sequencing to the genomics community. Genome Biol 2016;17(1):1146.

[20]Lu H, Giordano F, Ning Z. Oxford Nanopore MinION Sequencing and Genome Assembly. Genomics Proteomics Bioinformatics 2016;14(5):265–79.

[21]Brinkerhoff H, Kang ASW, Liu J, Aksimentiev A, Dekker C. Infinite re-reading of single proteins at single-amino-acid resolution using nanopore sequencing; 2021.

[22]Yan S, Zhang J, Wang Y, Guo W, Zhang S, Liu Y, Cao J, Wang Y, Wang L, Ma F, Zhang P, Chen H-Y, Huang S. Single Molecule Ratcheting Motion of Peptides in a Mycobacterium smegmatis Porin A (MspA) Nanopore. Nano Lett. 2021.

[23]Ouldali H, Sarthak K, Ensslen T, Piguet F, Manivet P, Pelta J, Behrends JC, Aksimentiev A, Oukhaled A. Electrical recognition of the twenty proteinogenic amino acids using an aerolysin nanopore. Nat Biotechnol 2020;38(2):176–81.

[24]Derrington IM, Butler TZ, Collins MD, Manrao E, Pavlenok M, Niederweis M, Gundlach JH. Nanopore DNA sequencing with MspA. Proceedings of the National Academy of Sciences 2010;107(37):16060–5.

[25]Hu Z-L, Huo M-Z, Ying Y-L, Long Y-T. Biological Nanopore Approach for Single-Molecule Protein Sequencing. Angew Chem Int Ed Engl 2021;60(27):14738–49.

[26]Freedman KJ, Otto LM, Ivanov AP, Barik A, Oh S-H, Edel JB. Nanopore sensing at ultra-low concentrations using single-molecule dielectrophoretic trapping. Nat Commun 2016;7(1).

[27]Cai S, Pataillot-Meakin T, Shibakawa A, Ren R, Bevan CL, Ladame S, Ivanov AP, Edel JB. Single-molecule amplification-free multiplexed detection of circulating microRNA cancer biomarkers from serum. Nat Commun 2021;12(1):3515.

[28]Höfler L, Gyurcsányi RE. Nanosensors lost in space. A random walk study of single molecule detection with single-nanopore sensors. Analytica Chimica Acta 2012;722:119–26.

[29]Karawdeniya BI, Bandara YMNDY, Nichols JW, Chevalier RB, Dwyer JR. Surveying silicon nitride nanopores for glycomics and heparin quality assurance. Nat Commun 2018;9(1):3278.

[30]Fang Z, Liu L, Wang Y, Xi D, Zhang S. Unambiguous Discrimination of Multiple Protein Biomarkers by Nanopore Sensing with Double-Stranded DNA-Based Probes. Anal. Chem. 2020;92(2):1730–7.

[31]Asandei A, Di Muccio G, Schiopu I, Mereuta L, Dragomir IS, Chinappi M, Luchian T. Nanopore-Based Protein Sequencing Using Biopores: Current Achievements and Open Challenges. Small Methods 2020;4(11):1900595.

[32]Drndić M. 20 years of solid-state nanopores. Nat Rev Phys 2021;3(9):606.

[33]Maitra RD, Kim J, Dunbar WB. Recent advances in nanopore sequencing. Electrophoresis 2012;33(23):3418–28.

[34]Liang S, Xiang F, Tang Z, Nouri R, He X, Dong M, Guan W. Noise in nanopore sensors: Sources, models, reduction, and benchmarking. Nanotechnology and Precision Engineering 2020;3(1):9–17.

[35]Fragasso A, Schmid S, Dekker C. Comparing Current Noise in Biological and Solid-State Nanopores. ACS Nano 2020;14(2):1338–49.

[36]Cressiot B, Bacri L, Pelta J. The Promise of Nanopore Technology: Advances in the Discrimination of Protein Sequences and Chemical Modifications. Small Methods 2020;4(11):2000090.

[37]Cressiot B, Ouldali H, Pastoriza-Gallego M, Bacri L, van der Goot FG, Pelta J. Aerolysin, a Powerful Protein Sensor for Fundamental Studies and Development of Upcoming Applications. ACS Sens. 2019;4(3):530–48.

[38]Asandei A, Rossini AE, Chinappi M, Park Y, Luchian T. Protein Nanopore-Based Discrimination between Selected Neutral Amino Acids from Polypeptides. Langmuir 2017;33(50):14451–9.

[39]Stefureac R, Waldner L, Howard P, Lee JS. Nanopore analysis of a small 86-residue protein. Small 2008;4(1):59–63.

[40]Stefureac RI, Lee JS. Nanopore Analysis of the Folding of Zinc Fingers. Small 2008;4(10):1646–50.

[41]Liu Z, Ghai I, Winterhalter M, Schwaneberg U. Engineering Enhanced Pore Sizes Using FhuA Δ1-160 from E. coli Outer Membrane as Template. ACS Sens. 2017;2(11):1619–26.

[42]Fried JP, Swett JL, Nadappuram BP, Mol JA, Edel JB, Ivanov AP, Yates JR. In situ solid-state nanopore fabrication. Chem. Soc. Rev. 2021;50(8):4974–92.

[43]Xue L, Yamazaki H, Ren R, Wanunu M, Ivanov AP, Edel JB. Solid-state nanopore sensors. Nat Rev Mater 2020;5(12):931–51.

[44]Su S, Wang X, Xue J. Nanopores in two-dimensional materials: accurate fabrication. Mater. Horiz. 2021;8(5):1390–408.

[45]Morris CA, Friedman AK, Baker LA. Applications of nanopipettes in the analytical sciences. Analyst 2010;135(9):2190–202.

[46]Stanley J, Pourmand N. Nanopipettes—The past and the present. APL Materials 2020;8(10):100902.

[47]Ma T, Janot J-M, Balme S. Track-Etched Nanopore/Membrane: From Fundamental to Applications. Small Methods 2020;4(9):2000366.

[48]Hu R, Tong X, Zhao Q. Four Aspects about Solid-State Nanopores for Protein Sensing: Fabrication, Sensitivity, Selectivity, and Durability. Adv. Healthcare Mater. 2020;9(17):e2000933.

[49]Das N, Mandal N, Sekhar PK, RoyChaudhuri C. Signal Processing for Single Biomolecule Identification Using Nanopores: A Review. IEEE Sensors Journal 2021;21(11):12808–20.

[50]Laucirica G, Terrones YT, Cayón V, Cortez ML, Toimil-Molares ME, Trautmann C, Marmisollé W, Azzaroni O. Biomimetic Solid-State Nanochannels for Chemical and Biological Sensing Applications. TrAC Trends in Analytical Chemistry 2021:116425.

[51]Zhang S, Chen W, Song L, Wang X, Sun W, Song P, Ashraf G, Liu B, Zhao Y-D. Recent advances in ionic current rectification based nanopore sensing: a mini-review. Sensors and Actuators Reports 2021;3:100042.

[52]Stein D, Li J, Golovchenko JA. Ion-Beam Sculpting Time Scales. Phys. Rev. Lett. 2002;89(27).

[53]Li J, Stein D, McMullan C, Branton D, Aziz MJ, Golovchenko JA. Ion-beam sculpting at nanometre length scales. Nature 2001;412(6843):166–9.

[54]Fischbein MD, Drndić M. Sub-10 nm Device Fabrication in a Transmission Electron Microscope. Nano Lett. 2007;7(5):1329–37.

[55]Larkin J, Henley R, Bell DC, Cohen-Karni T, Rosenstein JK, Wanunu M. Slow DNA transport through nanopores in hafnium oxide membranes. ACS Nano 2013;7(11):10121–8.

[56]Feng J, Liu K, Graf M, Dumcenco D, Kis A, Di Ventra M, Radenovic A. Observation of ionic Coulomb blockade in nanopores. Nature Mater 2016;15(8):850–5.

[57]Thiruraman JP, Masih Das P, Drndić M. Stochastic Ionic Transport in Single Atomic Zero-Dimensional Pores. ACS Nano 2020;14(9):11831–45.

[58]van den Hout M, Hall AR, Wu MY, Zandbergen HW, Dekker C, Dekker NH. Controlling nanopore size, shape and stability. Nanotechnology 2010;21(11):115304.

[59]Wanunu M, Meller A. Chemically modified solid-state nanopores. Nano Lett. 2007;7(6):1580–5.

[60]Roman J, Français O, Jarroux N, Patriarche G, Pelta J, Bacri L, Le Pioufle B. Solid-State Nanopore Easy Chip Integration in a Cheap and Reusable Microfluidic Device for Ion Transport and Polymer Conformation Sensing. ACS Sens. 2018;3(10):2129–37.

[61]Kwok H, Briggs K, Tabard-Cossa V. Nanopore fabrication by controlled dielectric breakdown. PLoS One 2014;9(3):e92880.

[62]Waugh M, Briggs K, Gunn D, Gibeault M, King S, Ingram Q, Jimenez AM, Berryman S, Lomovtsev D, Andrzejewski L, Tabard-Cossa V. Solid-state nanopore fabrication by automated controlled breakdown. Nat Protoc 2020;15(1):122–43.

[63]Ying C, Houghtaling J, Eggenberger OM, Guha A, Nirmalraj P, Awasthi S, Tian J, Mayer M. Formation of Single Nanopores with Diameters of 20-50 nm in Silicon Nitride Membranes Using Laser-Assisted Controlled Breakdown. ACS Nano 2018;12(11):11458–70.

[64]Wang Y, Ying C, Zhou W, Vreede L de, Liu Z, Tian J. Fabrication of multiple nanopores in a SiNx membrane via controlled breakdown. Sci Rep 2018;8(1):1234.

[65]Rangel EC, Gadioli GZ, Cruz NC. Investigations on the Stability of Plasma Modified Silicone Surfaces. Plasmas and Polymers 2004;9(1):35–48.

[66]Nagashima G, Levine EV, Hoogerheide DP, Burns MM, Golovchenko JA. Superheating and homogeneous single bubble nucleation in a solid-state nanopore. Phys. Rev. Lett. 2014;113(2):24506.

[67]Feng J, Liu K, Bulushev RD, Khlybov S, Dumcenco D, Kis A, Radenovic A. Identification of single nucleotides in MoS2 nanopores. Nature Nanotech 2015;10(12):1070–6.

[68]Merchant CA, Healy K, Wanunu M, Ray V, Peterman N, Bartel J, Fischbein MD, Venta K, Luo Z, Johnson ATC, Drndić M. DNA translocation through graphene nanopores. Nano Lett. 2010;10(8):2915–21.

[69]Zhou Z, Hu Y, Wang H, Xu Z, Wang W, Bai X, Shan X, Lu X. DNA translocation through hydrophilic nanopore in hexagonal boron nitride. Sci Rep 2013;3(1):3287.

[70]Feng J, Graf M, Liu K, Ovchinnikov D, Dumcenco D, Heiranian M, Nandigana V, Aluru NR, Kis A, Radenovic A. Single-layer MoS2 nanopores as nanopower generators. Nature 2016;536(7615):197–200.

[71]Mojtabavi M, VahidMohammadi A, Liang W, Beidaghi M, Wanunu M. Single-Molecule Sensing Using Nanopores in Two-Dimensional Transition Metal Carbide (MXene) Membranes. ACS Nano 2019;13(3):3042–53.

[72]Actis P, Mak AC, Pourmand N. Functionalized nanopipettes: toward label-free, single cell biosensors. Bioanal Rev 2010;1(2-4):177–85.

[73]Actis P, McDonald A, Beeler D, Vilozny B, Millhauser G, Pourmand N. Copper Sensing with a Prion Protein Modified Nanopipette. RSC Adv 2012;2(31):11638–40.

[74]Apel PY, Blonskaya IV, Dmitriev SN, Orelovich OL, Sartowska BA. Ion track symmetric and asymmetric nanopores in polyethylene terephthalate foils for versatile applications. Nuclear Instruments and Methods in Physics Research Section B: Beam Interactions with Materials and Atoms 2015;365:409–13.

[75]Apel P. Track etching technique in membrane technology. Radiation Measurements 2001;34(1-6):559–66.

[76]Apel PY, Korchev YE, Siwy Z, Spohr R, Yoshida M. Diode-like single-ion track membrane prepared by electro-stopping. Nuclear Instruments and Methods in Physics Research Section B: Beam Interactions with Materials and Atoms 2001;184(3):337–46.

[77]Ma T, Arroyo N, Marc Janot J, Picaud F, Balme S. Conformation of Polyethylene Glycol inside Confined Space: Simulation and Experimental Approaches. Nanomaterials (Basel) 2021;11(1):244.

[78]Lepoitevin M, Ma T, Bechelany M, Janot J-M, Balme S. Functionalization of single solid state nanopores to mimic biological ion channels: A review. Advances in Colloid and Interface Science 2017;250:195–213.

[79]An S, Jhe W. Nanopipette/Nanorod-Combined Quartz Tuning Fork–Atomic Force Microscope. Sensors (Basel) 2019;19(8).

[80]Ulrich N, Spende A, Burr L, Sobel N, Schubert I, Hess C, Trautmann C, Toimil-Molares ME. Conical Nanotubes Synthesized by Atomic Layer Deposition of Al2O3, TiO2, and SiO2 in Etched Ion-Track Nanochannels. Nanomaterials (Basel) 2021;11(8):1874.

[81]Apel PY, Blonskaya IV, Orelovitch OL, Dmitriev SN. Diode-like ion-track asymmetric nanopores: Some alternative methods of fabrication. Nuclear Instruments and Methods in Physics Research Section B: Beam Interactions with Materials and Atoms 2009;267(6):1023–7.

[82]Cervera J, Schiedt B, Neumann R, Mafé S, Ramírez P. Ionic conduction, rectification, and selectivity in single conical nanopores. The Journal of Chemical Physics 2006;124(10):104706.

[83]Siwy ZS. Ion-Current Rectification in Nanopores and Nanotubes with Broken Symmetry. Adv. Funct. Mater. 2006;16(6):735–46.

[84]Apel PY, Blonskaya IV, Orelovitch OL, Ramirez P, Sartowska BA. Effect of nanopore geometry on ion current rectification. Nanotechnology 2011;22(17):175302.

[85]Yameen B, Ali M, Neumann R, Ensinger W, Knoll W, Azzaroni O. Single Conical Nanopores Displaying pH-Tunable Rectifying Characteristics. Manipulating Ionic

Transport With Zwitterionic Polymer Brushes. J. Am. Chem. Soc. 2009;131(6):2070–1.

[86]White HS, Bund A. Ion Current Rectification at Nanopores in Glass Membranes. Langmuir 2008;24(5):2212–8.

[87]Siwy Z, Heins E, Harrell CC, Kohli P, Martin CR. Conical-Nanotube Ion-Current Rectifiers: The Role of Surface Charge. J. Am. Chem. Soc. 2004;126(35):10850–1.

[88]Macrae MX, Blake S, Mayer M, Yang J. Nanoscale Ionic Diodes with Tunable and Switchable Rectifying Behavior. J. Am. Chem. Soc. 2010;132(6):1766–7.

[89]Sa N, Lan W-J, Shi W, Baker LA. Rectification of ion current in nanopipettes by external substrates. ACS Nano 2013;7(12):11272–82.

[90]Ma T, Balanzat E, Janot J-M, Balme S. Single conical track-etched nanopore for a free-label detection of OSCS contaminants in heparin. Biosens Bioelectron 2019;137:207–12.

[91]Ali M, Yameen B, Cervera J, Ramírez P, Neumann R, Ensinger W, Knoll W, Azzaroni O. Layer-by-layer assembly of polyelectrolytes into ionic current rectifying solid-state nanopores: insights from theory and experiment. J. Am. Chem. Soc. 2010;132(24):8338–48.

[92]Lin C-Y, Ma T, Siwy ZS, Balme S, Hsu J-P. Tunable Current Rectification and Selectivity Demonstrated in Nanofluidic Diodes through Kinetic Functionalization. J Phys Chem Lett 2020;11(1):60–6.

[93]Zhao Y, Janot J-M, Balanzat E, Balme S. Mimicking pH-Gated Ionic Channels by Polyelectrolyte Complex Confinement Inside a Single Nanopore. Langmuir 2017;33(14):3484–90.

[94]Lepoitevin M, Jamilloux B, Bechelany M, Balanzat E, Janot J-M, Balme S. Fast and reversible functionalization of a single nanopore based on layer-by-layer polyelectrolyte self-assembly for tuning current rectification and designing sensors. RSC Adv 2016;6(38):32228–33.

[95]Ma T, Gaigalas P, Lepoitevin M, Plikusiene I, Bechelany M, Janot J-M, Balanzat E, Balme S. Impact of Polyelectrolyte Multilayers on the Ionic Current Rectification of Conical Nanopores. Langmuir 2018;34(11):3405–12.

[96]Actis P, Vilozny B, Seger RA, Li X, Jejelowo O, Rinaudo M, Pourmand N. Voltage-controlled metal binding on polyelectrolyte-functionalized nanopores. Langmuir 2011;27(10):6528–33.

[97]Balme S, Ma T, Balanzat E, Janot J-M. Large osmotic energy harvesting from functionalized conical nanopore suitable for membrane applications. Journal of Membrane Science 2017;544:18–24.

[98]Hou X, Zhang H, Jiang L. Building Bio-Inspired Artificial Functional Nanochannels: From Symmetric to Asymmetric Modification. Angew. Chem. Int. Ed. 2012;51(22):5296–307.

[99]Tian Y, Hou X, Jiang L. Biomimetic ionic rectifier systems: Asymmetric modification of single nanochannels by ion sputtering technology. Journal of Electroanalytical Chemistry 2011;656(1-2):231–6.

[100] Zhang Z, Kong X-Y, Xiao K, Xie G, Liu Q, Tian Y, Zhang H, Ma J, Wen L, Jiang L. A Bioinspired Multifunctional Heterogeneous Membrane with Ultrahigh Ionic Rectification and Highly Efficient Selective Ionic Gating. Adv. Mater. 2016;28(1):144–50.

[101] Ali M, Yameen B, Neumann R, Ensinger W, Knoll W, Azzaroni O. Biosensing and Supramolecular Bioconjugation in Single Conical Polymer Nanochannels. Facile Incorporation of Biorecognition Elements into Nanoconfined Geometries. J. Am. Chem. Soc. 2008;130(48):16351–7.

[102] Vlassiouk I, Kozel TR, Siwy ZS. Biosensing with Nanofluidic Diodes. J. Am. Chem. Soc. 2009;131(23):8211–20.

[103] Vlassiouk I, Siwy ZS. Nanofluidic Diode. Nano Lett. 2007;7(3):552–6.

[104] Ali M, Ramirez P, Tahir MN, Mafe S, Siwy Z, Neumann R, Tremel W, Ensinger W. Biomolecular conjugation inside synthetic polymer nanopores via glycoprotein-lectin interactions. Nanoscale 2011;3(4):1894–903.

[105] Cai S-L, Cao S-H, Zheng Y-B, Zhao S, Yang J-L, Li Y-Q. Surface charge modulated aptasensor in a single glass conical nanopore. Biosensors and Bioelectronics 2015;71:37–43.

[106] Actis P, Rogers A, Nivala J, Vilozny B, Seger RA, Jejelowo O, Pourmand N. Reversible thrombin detection by aptamer functionalized STING sensors. Biosensors and Bioelectronics 2011;26(11):4503–7.

[107] Pérez-Mitta G, Albesa AG, Trautmann C, Toimil-Molares ME, Azzaroni O. Bioinspired integrated nanosystems based on solid-state nanopores: “iontronic” transduction of biological, chemical and physical stimuli. Chem. Sci. 2017;8(2):890–913.

[108] Ali M, Ramirez P, Nguyen HQ, Nasir S, Cervera J, Mafe S, Ensinger W. Single cigar-shaped nanopores functionalized with amphoteric amino acid chains: experimental and theoretical characterization. ACS Nano 2012;6(4):3631–40.

[109] Ali M, Nasir S, Ensinger W. Stereoselective detection of amino acids with protein-modified single asymmetric nanopores. Electrochimica Acta 2016;215:231–7.

[110] Ali M, Bayer V, Schiedt B, Neumann R, Ensinger W. Fabrication and functionalization of single asymmetric nanochannels for electrostatic/hydrophobic association of protein molecules. Nanotechnology 2008;19(48):485711.

[111] Şen M, Demirci A. pH-Dependent ionic-current-rectification in nanopipettes modified with glutaraldehyde cross-linked protein membranes. RSC Adv 2016;6(89):86334–9.

[112] Reynaud L, Bouchet-Spinelli A, Raillon C, Buhot A. Sensing with Nanopores and Aptamers: A Way Forward. Sensors (Basel) 2020;20(16).

[113] Ali M, Nasir S, Ensinger W. Bioconjugation-induced ionic current rectification in aptamer-modified single cylindrical nanopores. Chem Commun (Camb) 2015;51(16):3454–7.

[114] Ali M, Nasir S, Ramirez P, Cervera J, Mafe S, Ensinger W. Carbohydrate-Mediated Biomolecular Recognition and Gating of Synthetic Ion Channels. J. Phys. Chem. C 2013;117(35):18234–42.

[115] Lepoitevin M, Nguyen G, Bechelany M, Balanzat E, Janot J-M, Balme S. Combining a sensor and a pH-gated nanopore based on an avidin-biotin system. Chem Commun (Camb) 2015;51(27):5994–7.

[116] Lepoitevin M, Bechelany M, Balanzat E, Janot J-M, Balme S. Non-Fluorescence label protein sensing with track-etched nanopore decorated by avidin/biotin system. Electrochimica Acta 2016;211:611–8.

[117] Duan L, Yobas L. Label-Free Multiplexed Electrical Detection of Cancer Markers on a Microchip Featuring an Integrated Fluidic Diode Nanopore Array. ACS Nano 2018;12(8):7892–900.

[118] Ali M, Nasir S, Ahmed I, Fruk L, Ensinger W. Tuning nanopore surface polarity and rectification properties through enzymatic hydrolysis inside nanoconfined geometries. Chem. Commun. 2013;49(78):8770–2.

[119] Ali M, Tahir MN, Siwy Z, Neumann R, Tremel W, Ensinger W. Hydrogen peroxide sensing with horseradish peroxidase-modified polymer single conical nanochannels. Anal Chem 2011;83(5):1673–80.

[120] Vilozny B, Actis P, Seger RA, Vallmajo-Martin Q, Pourmand N. Reversible cation response with a protein-modified nanopipette. Anal. Chem. 2011;83(16):6121–6.

[121] Pérez-Mitta G, Peinetti AS, Cortez ML, Toimil-Molares ME, Trautmann C, Azzaroni O. Highly Sensitive Biosensing with Solid-State Nanopores Displaying Enzymatically Reconfigurable Rectification Properties. Nano Lett. 2018;18(5):3303–10.

[122] KUBITSCHEK HE. Electronic Counting and Sizing of Bacteria. Nature 1958;182(4630):234–5.

[123] Bezrukov SM, Vodyanoy I. Probing alamethicin channels with water-soluble polymers. Effect on conductance of channel states. Biophysical Journal 1993;64(1):16–25.

[124] Kowalczyk SW, Dekker C. Measurement of the docking time of a DNA molecule onto a solid-state nanopore. Nano Lett. 2012;12(8):4159–63.

[125] Smeets RMM, Keyser UF, Krapf D, Wu M-Y, Dekker NH, Dekker C. Salt dependence of ion transport and DNA translocation through solid-state nanopores. Nano Lett. 2006;6(1):89–95.

[126] Japrung D, Dogan J, Freedman KJ, Nadzeyka A, Bauerdick S, Albrecht T, Kim MJ, Jemth P, Edel JB. Single-molecule studies of intrinsically disordered proteins using solid-state nanopores. Anal Chem 2013;85(4):2449–56.

[127] Yu R-J, Lu S-M, Xu S-W, Li Y-J, Xu Q, Ying Y-L, Long Y-T. Single molecule sensing of amyloid-β aggregation by confined glass nanopores. Chem. Sci. 2019;10(46):10728–32.

[128] Gu L-Q, Braha O, Conlan S, Cheley S, Bayley H. Stochastic sensing of organic analytes by a pore-forming protein containing a molecular adapter. Nature 1999;398(6729):686–90.

[129] Pulcu GS, Mikhailova E, Choi L-S, Bayley H. Continuous observation of the stochastic motion of an individual small-molecule walker. Nature Nanotech 2015;10(1):76–83.

[130] Lan W-J, Holden DA, Zhang B, White HS. Nanoparticle transport in conical-shaped nanopores. Anal Chem 2011;83(10):3840–7.

[131] Willmott GR. Tunable Resistive Pulse Sensing: Better Size and Charge Measurements for Submicrometer Colloids. Anal. Chem. 2018;90(5):2987–95.

[132] Vogel R, Anderson W, Eldridge J, Glossop B, Willmott G. A Variable Pressure Method for Characterizing Nanoparticle Surface Charge Using Pore Sensors. Anal. Chem. 2012;84(7):3125–31.

[133] Coglitore D, Merenda A, Giamblanco N, Dumée LF, Janot J-M, Balme S. Metal alloy solid-state nanopores for single nanoparticle detection. Phys Chem Chem Phys 2018;20(18):12799–807.

[134] Platt M, Maugi R. Incorporating Peptide Aptamers into Resistive Pulse Sensing; 2019.

[135] Zhao Q, Zoysa RSS de, Wang D, Jayawardhana DA, Guan X. Real-time monitoring of peptide cleavage using a nanopore probe. J Am Chem Soc 2009;131(18):6324–5.

[136] Piguet F, Ouldali H, Pastoriza-Gallego M, Manivet P, Pelta J, Oukhaled A. Identification of single amino acid differences in uniformly charged homopolymeric peptides with aerolysin nanopore. Nat Commun 2018;9(1).

[137] Restrepo-Pérez L, Huang G, Bohländer PR, Worp N, Eelkema R, Maglia G, Joo C, Dekker C. Resolving Chemical Modifications to a Single Amino Acid within a Peptide Using a Biological Nanopore. ACS Nano 2019;13(12):13668–76.

[138] Yusko EC, Johnson JM, Majd S, Prangkio P, Rollings RC, Li J, Yang J, Mayer M. Controlling protein translocation through nanopores with bio-inspired fluid walls. Nature Nanotech 2011;6(4):253–60.

[139] Balme S, Coulon PE, Lepoitevin M, Charlot B, Yandrapalli N, Favard C, Muriaux D, Bechelany M, Janot J-M. Influence of Adsorption on Proteins and Amyloid Detection by Silicon Nitride Nanopore. Langmuir 2016;32(35):8916–25.

[140] Plesa C, Kowalczyk SW, Zinsmeester R, Grosberg AY, Rabin Y, Dekker C. Fast translocation of proteins through solid state nanopores. Nano Lett 2013;13(2):658–63.

[141] Waduge P, Hu R, Bandarkar P, Yamazaki H, Cressiot B, Zhao Q, Whitford PC, Wanunu M. Nanopore-Based Measurements of Protein Size, Fluctuations, and Conformational Changes. ACS Nano 2017;11(6):5706–16.

[142] Yusko EC, Prangkio P, Sept D, Rollings RC, Li J, Mayer M. Single-Particle Characterization of Aβ Oligomers in Solution. ACS Nano 2012;6(7):5909–19.

[143] Giamblanco N, Coglitore D, Janot J-M, Coulon PE, Charlot B, Balme S. Detection of protein aggregate morphology through single antifouling nanopore. Sensors and Actuators B: Chemical 2018;260:736–45.

[144] Madampage CA, Tavassoly O, Christensen C, Kumari M, Lee JS. Nanopore analysis. Prion 2012;6(2):116–23.

[145] Yang L, Yamamoto T. Quantification of Virus Particles Using Nanopore-Based Resistive-Pulse Sensing Techniques. Front. Microbiol. 2016;7.

[146] Arima A, Tsutsui M, Harlisa IH, Yoshida T, Tanaka M, Yokota K, Tonomura W, Taniguchi M, Okochi M, Washio T, Kawai T. Selective detections of single-viruses using solid-state nanopores. Sci Rep 2018;8(1):16305.

[147] Taniguchi M, Minami S, Ono C, Hamajima R, Morimura A, Hamaguchi S, Akeda Y, Kanai Y, Kobayashi T, Kamitani W, Terada Y, Suzuki K, Hatori N, Yamagishi Y, Washizu N, Takei H, Sakamoto O, Naono N, Tatematsu K, Washio T, Matsuura Y, Tomono K. Combining machine learning and nanopore construction creates an artificial intelligence nanopore for coronavirus detection. Nat Commun 2021;12(1):3726.

[148] Coglitore D, Giamblanco N, Kizalaité A, Coulon PE, Charlot B, Janot J-M, Balme S. Unexpected Hard Protein Behavior of BSA on Gold Nanoparticle Caused by Resveratrol. Langmuir 2018;34(30):8866–74.

[149] Coglitore D, Coulon PE, Janot J-M, Balme S. Revealing the Nanoparticle-Protein Corona with a Solid-State Nanopore. Materials (Basel) 2019;12(21).

[150] Eggenberger OM, Ying C, Mayer M. Surface coatings for solid-state nanopores. Nanoscale 2019;11(42):19636–57.

[151] Giamblanco N, Coglitore D, Gubbiotti A, Ma T, Balanzat E, Janot J-M, Chinappi M, Balme S. Amyloid Growth, Inhibition, and Real-Time Enzymatic Degradation Revealed with Single Conical Nanopore. Anal. Chem. 2018;90(21):12900–8.

[152] Meyer N, Arroyo N, Janot J-M, Lepoitevin M, Stevenson A, Nemeir IA, Perrier V, Bougard D, Belondrade M, Cot D, Bentin J, Picaud F, Torrent J, Balme S. Detection of Amyloid-β Fibrils Using Track-Etched Nanopores: Effect of Geometry and Crowding. ACS Sens. 2021;6(10):3733–43.

[153] Freedman KJ, Haq SR, Edel JB, Jemth P, Kim MJ. Single molecule unfolding and stretching of protein domains inside a solid-state nanopore by electric field. Sci Rep 2013;3:1638.

[154] Oukhaled A, Cressiot B, Bacri L, Pastoriza-Gallego M, Betton J-M, Bourhis E, Jede R, Gierak J, Auvray L, Pelta J. Dynamics of completely unfolded and native proteins through solid-state nanopores as a function of electric driving force. ACS Nano 2011;5(5):3628–38.

[155] Bezrukov SM. Ion channels as molecular coulter counters to probe metabolite transport. J Membr Biol 2000;174(1):1–13.

[156] Henriquez RR, Ito T, Sun L, Crooks RM. The resurgence of Coulter counting for analyzing nanoscale objects. Analyst 2004;129(6):478–82.

[157] Talaga DS, Li J. Single-molecule protein unfolding in solid state nanopores. J Am Chem Soc 2009;131(26):9287–97.

[158] Qin Z, Zhe J, Wang G-X. Effects of particle's off-axis position, shape, orientation and entry position on resistance changes of micro Coulter counting devices. Meas. Sci. Technol. 2011;22(4):45804.

[159] Smythe WR. Flow Around a Spheroid in a Circular Tube. Phys. Fluids 1964;7(5):633.

[160] DeBlois RW, Bean CP. Counting and Sizing of Submicron Particles by the Resistive Pulse Technique. Review of Scientific Instruments 1970;41(7):909–16.

[161] Han A, Creus M, Schürmann G, Linder V, Ward TR, Rooij NF de, Staufer U. Label-free detection of single protein molecules and protein-protein interactions using synthetic nanopores. Anal Chem 2008;80(12):4651–8.

[162] Ito T, Sun L, Crooks RM. Simultaneous determination of the size and surface charge of individual nanoparticles using a carbon nanotube-based Coulter counter. Anal Chem 2003;75(10):2399–406.

[163] DeBlois RW, Uzgiris EE, Cluxton DH, Mazzone HM. Comparative measurements of size and polydispersity of several insect viruses. Anal Biochem 1978;90(1):273–88.

[164] Han X, Jin M, Breuker K, McLafferty FW. Extending top-down mass spectrometry to proteins with masses greater than 200 kilodaltons. Science 2006;314(5796):109–12.

[165] Wei R, Gatterdam V, Wieneke R, Tampé R, Rant U. Stochastic sensing of proteins with receptor-modified solid-state nanopores. Nat Nanotechnol 2012;7(4):257–63.

[166] Soni GV, Dekker C. Detection of nucleosomal substructures using solid-state nanopores. Nano Lett 2012;12(6):3180–6.

[167] Raillon C, Cousin P, Traversi F, Garcia-Cordero E, Hernandez N, Radenovic A. Nanopore detection of single molecule RNAP-DNA transcription complex. Nano Lett 2012;12(3):1157–64.

[168] Fologea D, Ledden B, McNabb DS, Li J. Electrical characterization of protein molecules by a solid-state nanopore. Appl Phys Lett 2007;91(5):539011–3.

[169] Lan W-J, Kubeil C, Xiong J-W, Bund A, White HS. Effect of Surface Charge on the Resistive Pulse Waveshape during Particle Translocation through Glass Nanopores. J. Phys. Chem. C 2014;118(5):2726–34.

[170] Varongchayakul N, Huttner D, Grinstaff MW, Meller A. Sensing Native Protein Solution Structures Using a Solid-state Nanopore: Unraveling the States of VEGF. Sci Rep 2018;8(1):1017.

[171] Hurley J. Sizing particles with a Coulter counter. Biophysical Journal 1970;10(1):74–9.

[172] Liu H, Qian S, Bau HH. The effect of translocating cylindrical particles on the ionic current through a nanopore. Biophysical Journal 2007;92(4):1164–77.

[173] Golibersuch DC. Observation of Aspherical Particle Rotation in Poiseuille Flow via the Resistance Pulse Technique. Biophysical Journal 1973;13(3):265–80.

[174] Fricke H. A MATHEMATICAL TREATMENT OF THE ELECTRICAL CONDUCTIVITY OF COLLOIDS AND CELL SUSPENSIONS. J Gen Physiol 1924;6(4):375–84.

[175] Berge LI, Feder J, Jo/ssang T. A novel method to study single-particle dynamics by the resistive pulse technique. Review of Scientific Instruments 1989;60(8):2756–63.

[176] Holden MA, Needham D, Bayley H. Functional bionetworks from nanoliter water droplets. J Am Chem Soc 2007;129(27):8650–5.

[177] Yusko EC, Bruhn BR, Eggenberger OM, Houghtaling J, Rollings RC, Walsh NC, Nandivada S, Pindrus M, Hall AR, Sept D, Li J, Kalonia DS, Mayer M. Real-time shape approximation and fingerprinting of single proteins using a nanopore. Nature Nanotech 2017;12(4):360–7.

[178] Houghtaling J, Ying C, Eggenberger OM, Fennouri A, Nandivada S, Acharjee M, Li J, Hall AR, Mayer M. Estimation of Shape, Volume, and Dipole Moment of Individual Proteins Freely Transiting a Synthetic Nanopore. ACS Nano 2019;13(5):5231–42.

[179] Pedone D, Firnkes M, Rant U. Data analysis of translocation events in nanopore experiments. Anal. Chem. 2009;81(23):9689–94.

[180] Firnkes M, Pedone D, Knezevic J, Döblinger M, Rant U. Electrically facilitated translocations of proteins through silicon nitride nanopores: conjoint and competitive action of diffusion, electrophoresis, and electroosmosis. Nano Lett 2010;10(6):2162–7.

[181] Larkin J, Henley RY, Muthukumar M, Rosenstein JK, Wanunu M. High-bandwidth protein analysis using solid-state nanopores. Biophysical Journal 2014;106(3):696–704.

[182] Balme S, Lepoitevin M, Dumée LF, Bechelany M, Janot J-M. Diffusion dynamics of latex nanoparticles coated with ssDNA across a single nanopore. Soft Matter 2017;13(2):496–502.

[183] Cressiot B, Oukhaled A, Patriarche G, Pastoriza-Gallego M, Betton J-M, Auvray L, Muthukumar M, Bacri L, Pelta J. Protein Transport through a Narrow Solid-State Nanopore at High Voltage: Experiments and Theory. ACS Nano 2012;6(7):6236–43.

[184] Sexton LT, Mukaibo H, Katira P, Hess H, Sherrill SA, Horne LP, Martin CR. An adsorption-based model for pulse duration in resistive-pulse protein sensing. J Am Chem Soc 2010;132(19):6755–63.

[185] Coglitore D, Janot J-M, Balme S. Protein at liquid solid interfaces: Toward a new paradigm to change the approach to design hybrid protein/solid-state materials. Advances in Colloid and Interface Science 2019;270:278–92.

[186] Roman J, Jarroux N, Patriarche G, Français O, Pelta J, Le Pioufle B, Bacri L. Functionalized Solid-State Nanopore Integrated in a Reusable Microfluidic Device for a Better Stability and Nanoparticle Detection. ACS Appl. Mater. Interfaces 2017;9(48):41634–40.

[187] Yu S, Lee SB, Kang M, Martin CR. Size-Based Protein Separations in Poly(ethylene glycol)-Derivatized Gold Nanotubule Membranes. Nano Lett. 2001;1(9):495–8.

[188] Arroyo N, Balme S, Picaud F. Impact of surface state on polyethylene glycol conformation confined inside a nanopore. The Journal of Chemical Physics 2021;154(10):104901.

[189] Hu R, Diao J, Li J, Tang Z, Li X, Leitz J, Long J, Liu J, Yu D, Zhao Q. Intrinsic and membrane-facilitated α-synuclein oligomerization revealed by label-free detection through solid-state nanopores. Sci Rep 2016;6(1).

[190] Eggenberger OM, Leriche G, Koyanagi T, Ying C, Houghtaling J, Schroeder TBH, Yang J, Li J, Hall A, Mayer M. Fluid surface coatings for solid-state nanopores:

comparison of phospholipid bilayers and archaea-inspired lipid monolayers. Nanotechnology 2019;30(32):325504.

[191] Hernández-Ainsa S, Muus C, Bell NAW, Steinbock LJ, Thacker VV, Keyser UF. Lipid-coated nanocapillaries for DNA sensing. Analyst 2013;138(1):104–6.

[192] Awasthi S, Sriboonpeng P, Ying C, Houghtaling J, Shorubalko I, Marion S, Davis SJ, Sola L, Chiari M, Radenovic A, Mayer M. Polymer Coatings to Minimize Protein Adsorption in Solid-State Nanopores. Small Methods 2020;4(11):2000177.

[193] Nir I, Huttner D, Meller A. Direct Sensing and Discrimination among Ubiquitin and Ubiquitin Chains Using Solid-State Nanopores. Biophysical Journal 2015;108(9):2340–9.

[194] Huang G, Willems K, Soskine M, Wloka C, Maglia G. Electro-osmotic capture and ionic discrimination of peptide and protein biomarkers with FraC nanopores. Nat Commun 2017;8(1).

[195] Di Fiori N, Squires A, Bar D, Gilboa T, Moustakas TD, Meller A. Optoelectronic control of surface charge and translocation dynamics in solid-state nanopores. Nature Nanotech 2013;8(12):946–51.

[196] Kim H-J, Choi U-J, Kim H, Lee K, Park K-B, Kim H-M, Kwak D-K, Chi S-W, Lee JS, Kim K-B. Translocation of DNA and protein through a sequentially polymerized polyurea nanopore. Nanoscale 2019;11(2):444–53.

[197] Zhang Y, Zhao J, Si W, Kan Y, Xu Z, Sha J, Chen Y. Electroosmotic Facilitated Protein Capture and Transport through Solid-State Nanopores with Diameter Larger than Length. Small Methods 2020;4(11):1900893.

[198] Sze JYY, Ivanov AP, Cass AEG, Edel JB. Single molecule multiplexed nanopore protein screening in human serum using aptamer modified DNA carriers. Nat Commun 2017;8(1):1552.

[199] Bell NAW, Keyser UF. Digitally encoded DNA nanostructures for multiplexed, single-molecule protein sensing with nanopores. Nat Nanotechnol 2016;11(7):645–51.

[200] Bell NAW, Thacker VV, Hernández-Ainsa S, Fuentes-Perez ME, Moreno-Herrero F, Liedl T, Keyser UF. Multiplexed ionic current sensing with glass nanopores. Lab Chip 2013;13(10):1859.

[201] Kowalczyk SW, Hall AR, Dekker C. Detection of local protein structures along DNA using solid-state nanopores. Nano Lett. 2010;10(1):324–8.

[202] Park K-B, Kim H-J, Kim H-M, Han SA, Lee KH, Kim S-W, Kim K-B. Noise and sensitivity characteristics of solid-state nanopores with a boron nitride 2-D membrane on a pyrex substrate. Nanoscale 2016;8(10):5755–63.

[203] Dimitrov V, Mirsaidov U, Wang D, Sorsch T, Mansfield W, Miner J, Klemens F, Cirelli R, Yemenicioglu S, Timp G. Nanopores in solid-state membranes engineered for single molecule detection. Nanotechnology 2010;21(6):65502.

[204] Uram JD, Ke K, Mayer M. Noise and bandwidth of current recordings from submicrometer pores and nanopores. ACS Nano 2008;2(5):857–72.

[205] Chen P, Gu J, Brandin E, Kim Y-R, Wang Q, Branton D. PROBING SINGLE DNA MOLECULE TRANSPORT USING FABRICATED NANOPORES. Nano Lett. 2004;4(11):2293–8.

[206] Chen P, Mitsui T, Farmer DB, Golovchenko J, Gordon RG, Branton D. Atomic Layer Deposition to Fine-Tune the Surface Properties and Diameters of Fabricated Nanopores. Nano Lett. 2004;4(7):1333–7.

[207] Thangaraj V, Lepoitevin M, Smietana M, Balanzat E, Bechelany M, Janot J-M, Vasseur J-J, Subramanian S, Balme S. Detection of short ssDNA and dsDNA by current-voltage measurements using conical nanopores coated with Al2O3 by atomic layer deposition. Microchim Acta 2016;183(3):1011–7.

[208] Li W, Bell NAW, Hernández-Ainsa S, Thacker VV, Thackray AM, Bujdoso R, Keyser UF. Single protein molecule detection by glass nanopores. ACS Nano 2013;7(5):4129–34.

[209] Beamish E, Kwok H, Tabard-Cossa V, Godin M. Fine-tuning the size and minimizing the noise of solid-state nanopores. J Vis Exp 2013;(80):e51081.

[210] Tabard-Cossa V, Trivedi D, Wiggin M, Jetha NN, Marziali A. Noise analysis and reduction in solid-state nanopores. Nanotechnology 2007;18(30):305505.

[211] Lee M-H, Kumar A, Park K-B, Cho S-Y, Kim H-M, Lim M-C, Kim Y-R, Kim K-B. A low-noise solid-state nanopore platform based on a highly insulating substrate. Sci Rep 2014;4(1):7448.

[212] Balan A, Machielse B, Niedzwiecki D, Lin J, Ong P, Engelke R, Shepard KL, Drndić M. Improving signal-to-noise performance for DNA translocation in solid-state nanopores at MHz bandwidths. Nano Lett. 2014;14(12):7215–20.

[213] Hu R, Rodrigues JV, Waduge P, Yamazaki H, Cressiot B, Chishti Y, Makowski L, Yu D, Shakhnovich E, Zhao Q, Wanunu M. Differential Enzyme Flexibility Probed Using Solid-State Nanopores. ACS Nano 2018;12(5):4494–502.

[214] Chae H, Kwak D-K, Lee M-K, Chi S-W, Kim K-B. Solid-state nanopore analysis on conformation change of p53TAD-MDM2 fusion protein induced by protein-protein interaction. Nanoscale 2018;10(36):17227–35.

[215] Waugh M, Carlsen A, Sean D, Slater GW, Briggs K, Kwok H, Tabard-Cossa V. Interfacing solid-state nanopores with gel media to slow DNA translocations. Electrophoresis 2015;36(15):1759–67.

[216] Tang Z, Liang Z, Lu B, Li J, Hu R, Zhao Q, Yu D. Gel mesh as "brake" to slow down DNA translocation through solid-state nanopores. Nanoscale 2015;7(31):13207–14.

[217] Squires AH, Hersey JS, Grinstaff MW, Meller A. A nanopore-nanofiber mesh biosensor to control DNA translocation. J. Am. Chem. Soc. 2013;135(44):16304–7.

[218] Acharya S, Jiang A, Kuo C, Nazarian R, Li K, Ma A, Siegal B, Toh C, Schmidt JJ. Improved Measurement of Proteins Using a Solid-State Nanopore Coupled with a Hydrogel. ACS Sens. 2020;5(2):370–6.

[219] Chau CC, Radford SE, Hewitt EW, Actis P. Macromolecular Crowding Enhances the Detection of DNA and Proteins by a Solid-State Nanopore. Nano Lett. 2020;20(7):5553–61.

[220] Al Sulaiman D, Chang JYH, Bennett NR, Topouzi H, Higgins CA, Irvine DJ, Ladame S. Hydrogel-Coated Microneedle Arrays for Minimally Invasive Sampling and Sensing of Specific Circulating Nucleic Acids from Skin Interstitial Fluid. ACS Nano 2019;13(8):9620–8.

[221] Reynaud L, Bouchet-Spinelli A, Janot J-M, Buhot A, Balme S, Raillon C. Discrimination of α-Thrombin and γ-Thrombin Using Aptamer-Functionalized Nanopore Sensing. Anal. Chem. 2021;93(22):7889–97.

[222] Smith MA, Ersavas T, Ferguson JM, Liu H, Lucas MC, Begik O, Bojarski L, Barton K, Novoa EM. Barcoding and demultiplexing Oxford Nanopore native RNA sequencing reads with deep residual learning; 2019.

[223] Landry M, Winters-Hilt S. Analysis of nanopore detector measurements using Machine-Learning methods, with application to single-molecule kinetic analysis. BMC Bioinformatics 2007;8 Suppl 7:S12.

[224] Meyer N, Janot J-M, Lepoitevin M, Smietana M, Vasseur J-J, Torrent J, Balme S. Machine Learning to Improve the Sensing of Biomolecules by Conical Track-Etched Nanopore. Biosensors (Basel) 2020;10(10).

[225] Namuduri S, Narayanan BN, Davuluru VSP, Burton L, Bhansali S. Review—Deep Learning Methods for Sensor Based Predictive Maintenance and Future Perspectives for Electrochemical Sensors. J. Electrochem. Soc. 2020;167(3):37552.

[226] Im J, Lindsay S, Wang X, Zhang P. Single Molecule Identification and Quantification of Glycosaminoglycans Using Solid-State Nanopores. ACS Nano 2019;13(6):6308–18.

[227] Xia K, Hagan JT, Fu L, Sheetz BS, Bhattacharya S, Zhang F, Dwyer JR, Linhardt RJ. Synthetic heparan sulfate standards and machine learning facilitate the development of solid-state nanopore analysis. Proc Natl Acad Sci USA 2021;118(11):e2022806118.

[228] Arima A, Tsutsui M, Washio T, Baba Y, Kawai T. Solid-State Nanopore Platform Integrated with Machine Learning for Digital Diagnosis of Virus Infection. Anal Chem 2021;93(1):215–27.

[229] Hattori S, Sekido R, Leong IW, Tsutsui M, Arima A, Tanaka M, Yokota K, Washio T, Kawai T, Okochi M. Machine learning-driven electronic identifications of single pathogenic bacteria. Sci Rep 2020;10(1):15525.

[230] Arima A, Harlisa IH, Yoshida T, Tsutsui M, Tanaka M, Yokota K, Tonomura W, Yasuda J, Taniguchi M, Washio T, Okochi M, Kawai T. Identifying Single Viruses Using Biorecognition Solid-State Nanopores. J. Am. Chem. Soc. 2018;140(48):16834–41.

[231] Yu J-S, Hong SC, Wu S, Kim H-M, Lee C, Lee J-S, Lee JE, Kim K-B. Differentiation of selectively labeled peptides using solid-state nanopores. Nanoscale 2019;11(5):2510–20.

[232] Umehara S, Pourmand N, Webb CD, Davis RW, Yasuda K, Karhanek M. Current rectification with poly-l-lysine-coated quartz nanopipettes. Nano Lett. 2006;6(11):2486–92.

[233] Li Q, Ying Y-L, Liu S-C, Lin Y, Long Y-T. Detection of Single Proteins with a General Nanopore Sensor. ACS Sens. 2019;4(5):1185–9.

[234] Fanzio P, Mussi V, Menotta M, Firpo G, Repetto L, Guida P, Angeli E, Magnani M, Valbusa U. Selective protein detection with a dsLNA-functionalized nanopore. Biosens Bioelectron 2015;64:219–26.

[235] Fujinami Tanimoto IM, Cressiot B, Jarroux N, Roman J, Patriarche G, Le Pioufle B, Pelta J, Bacri L. Selective target protein detection using a decorated nanopore into a microfluidic device. Biosens Bioelectron 2021;183:113195.

[236] Sexton LT, Horne LP, Martin CR. Developing synthetic conical nanopores for biosensing applications. Mol Biosyst 2007;3(10):667–85.

[237] Wharton JE, Jin P, Sexton LT, Horne LP, Sherrill SA, Mino WK, Martin CR. A method for reproducibly preparing synthetic nanopores for resistive-pulse biosensors. Small 2007;3(8):1424–30.

[238] Sexton LT, Horne LP, Sherrill SA, Bishop GW, Baker LA, Martin CR. Resistive-pulse studies of proteins and protein/antibody complexes using a conical nanotube sensor. J Am Chem Soc 2007;129(43):13144–52.

[239] Wang C, Fu Q, Wang X, Kong D, Sheng Q, Wang Y, Chen Q, Xue J. Atomic layer deposition modified track-etched conical nanochannels for protein sensing. Anal Chem 2015;87(16):8227–33.

[240] Steinbock LJ, Krishnan S, Bulushev RD, Borgeaud S, Blokesch M, Feletti L, Radenovic A. Probing the size of proteins with glass nanopores. Nanoscale 2014;6(23):14380–7.

[241] Ying Y-L, Yu R-J, Hu Y-X, Gao R, Long Y-T. Single antibody-antigen interactions monitored via transient ionic current recording using nanopore sensors. Chem. Commun. 2017;53(61):8620–3.

[242] Barati Farimani A, Heiranian M, Min K, Aluru NR. Antibody Subclass Detection Using Graphene Nanopores. J Phys Chem Lett 2017;8(7):1670–6.

[243] Freedman KJ, Jürgens M, Prabhu A, Ahn CW, Jemth P, Edel JB, Kim MJ. Chemical, thermal, and electric field induced unfolding of single protein molecules studied using nanopores. Anal Chem 2011;83(13):5137–44.

[244] Restrepo-Pérez L, John S, Aksimentiev A, Joo C, Dekker C. SDS-assisted protein transport through solid-state nanopores. Nanoscale 2017;9(32):11685–93.

[245] Saharia J, Bandara YMNDY, Lee JS, Wang Q, Kim MJ, Kim MJ. Fabrication of hexagonal boron nitride based 2D nanopore sensor for the assessment of electro-chemical responsiveness of human serum transferrin protein. Electrophoresis 2020;41(7-8):630–7.

[246] Lee K, Park K-B, Kim H-J, Yu J-S, Chae H, Kim H-M, Kim K-B. Recent Progress in Solid-State Nanopores. Advanced Materials 2018;30(42):e1704680.

[247] Wu Y, Yao Y, Cheong S, Tilley RD, Gooding JJ. Selectively detecting attomolar concentrations of proteins using gold lined nanopores in a nanopore blockade sensor. Chem. Sci. 2020.

[248] N. Das, R. Ray, S. Ray, C. Roychaudhuri. Intelligent Quantification of Picomolar Protein Concentration in Serum by Functionalized Nanopores. IEEE Sensors Journal 2018;18(24):10183–91.

[249] Li X, Tong X, Lu W, Yu D, Diao J, Zhao Q. Label-free detection of early oligomerization of α-synuclein and its mutants A30P/E46K through solid-state nanopores. Nanoscale 2019;11(13):6480–8.

[250] Martyushenko N, Bell NAW, Lamboll RD, Keyser UF. Nanopore analysis of amyloid fibrils formed by lysozyme aggregation. Analyst 2015;140(14):4882–6.

[251] Giamblanco N, Fichou Y, Janot J-M, Balanzat E, Han S, Balme S. Mechanisms of Heparin-Induced Tau Aggregation Revealed by a Single Nanopore. ACS Sens. 2020;5(4):1158–67.

[252] Giamblanco N, Janot J-M, Gubbiotti A, Chinappi M, Balme S. Characterization of Food Amyloid Protein Digestion by Conical Nanopore. Small Methods 2020;4(11):1900703.

[253] Ma T, Janot J-M, Balme S. Dynamics of long hyaluronic acid chains through conical nanochannels for characterizing enzyme reactions in confined spaces. Nanoscale 2020;12(13):7231–9.

[254] Sun L, Shigyou K, Ando T, Watanabe S. Thermally Driven Approach To Fill Sub-10-nm Pipettes with Batch Production. Anal. Chem. 2019;91(21):14080–4.

[255] Salançon E, Tinland B. Filling nanopipettes with apertures smaller than 50 nm: dynamic microdistillation. Beilstein J Nanotechnol 2018;9:2181–7.

[256] Balme S, Picaud F, Manghi M, Palmeri J, Bechelany M, Cabello-Aguilar S, Abou-Chaaya A, Miele P, Balanzat E, Janot JM. Ionic transport through sub-10 nm diameter hydrophobic high-aspect ratio nanopores: experiment, theory and simulation. Sci Rep 2015;5(1):10135.

[257] Chinappi M, Cecconi F. Protein sequencing via nanopore based devices: a nanofluidics perspective. J Phys Condens Matter 2018;30(20):204002.

[258] Alfaro JA, Bohländer P, Dai M, Filius M, Howard CJ, van Kooten XF, Ohayon S, Pomorski A, Schmid S, Aksimentiev A, Anslyn EV, Bedran G, Cao C, Chinappi M, Coyaud E, Dekker C, Dittmar G, Drachman N, Eelkema R, Goodlett D, Hentz S, Kalathiya U, Kelleher NL, Kelly RT, Kelman Z, Kim SH, Kuster B, Rodriguez-Larrea D, Lindsay S, Maglia G, Marcotte EM, Marino JP, Masselon C, Mayer M, Samaras P, Sarthak K, Sepiashvili L, Stein D, Wanunu M, Wilhelm M, Yin P, Meller A, Joo C. The emerging landscape of single-molecule protein sequencing technologies. Nat Methods 2021;18(6):604–17.

[259] Restrepo-Pérez L, Joo C, Dekker C. Paving the way to single-molecule protein sequencing. Nature Nanotech 2018;13(9):786–96.

[260] Lucas FLR, Versloot RCA, Yakovlieva L, Walvoort MTC, Maglia G. Protein identification by nanopore peptide profiling. Nat Commun 2021;12(1):5795.

[261] Chen H, Li L, Zhang T, Qiao Z, Tang J, Zhou J. Protein Translocation through a MoS 2 Nanopore:A Molecular Dynamics Study. J. Phys. Chem. C 2018;122(4):2070–80.

[262] Luan B, Zhou R. Single-File Protein Translocations through Graphene-MoS2 Heterostructure Nanopores. J Phys Chem Lett 2018;9(12):3409–15.